

Failure Modes and Mechanics of Fracture in Co-Fired Engineering Ceramics- LTCC

SAND2017-5344C

Rajan Tandon, Clay Newton

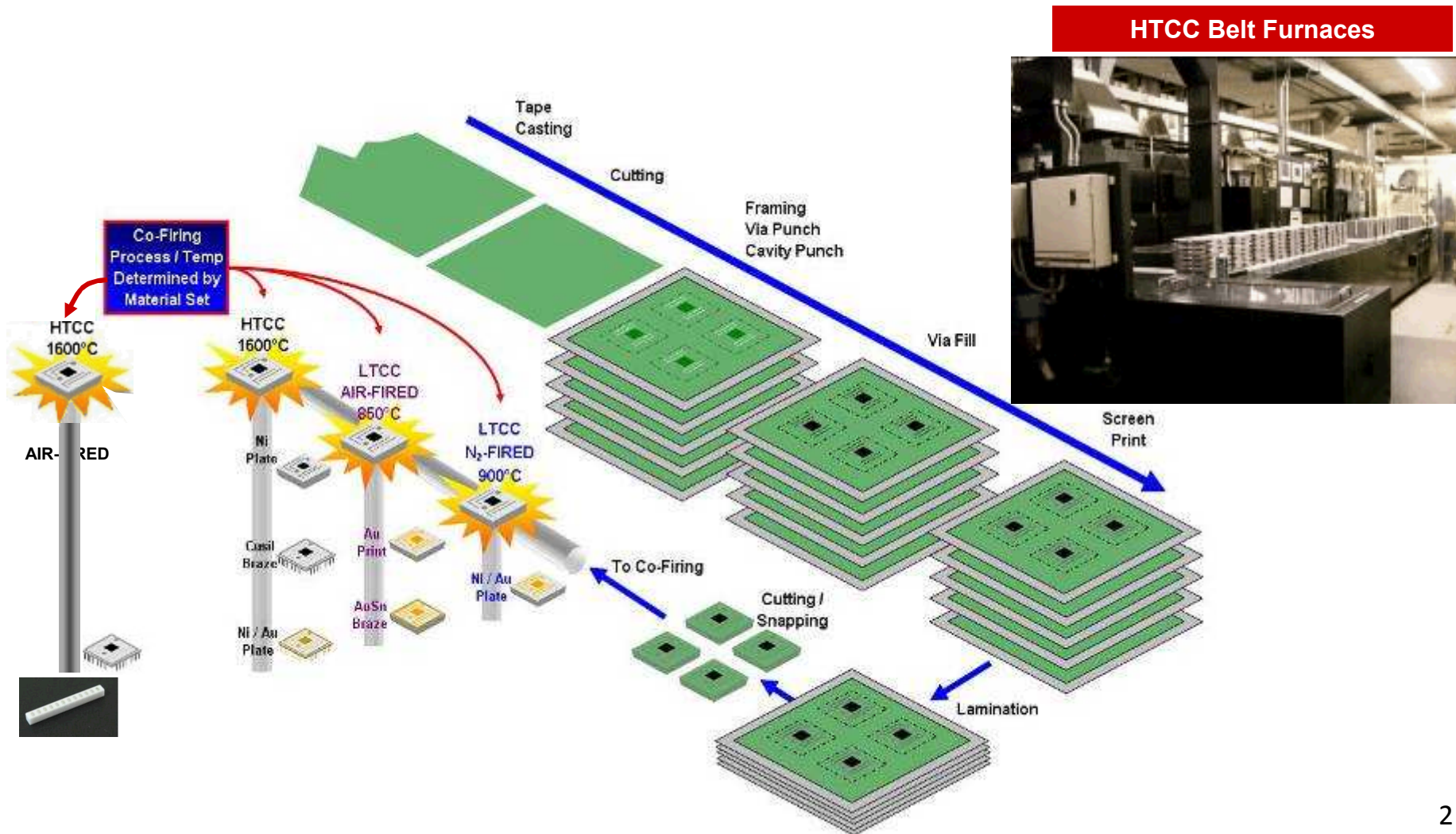
Sandia National Laboratories, Albuquerque, NM



Sandia National Laboratories is a multi-mission laboratory managed and operated by National Technology and Engineering Solutions of Sandia, LLC., a wholly owned subsidiary of Honeywell International, Inc., for the U.S. Department of Energy's National Nuclear Security Administration under contract DE-NA0003525.

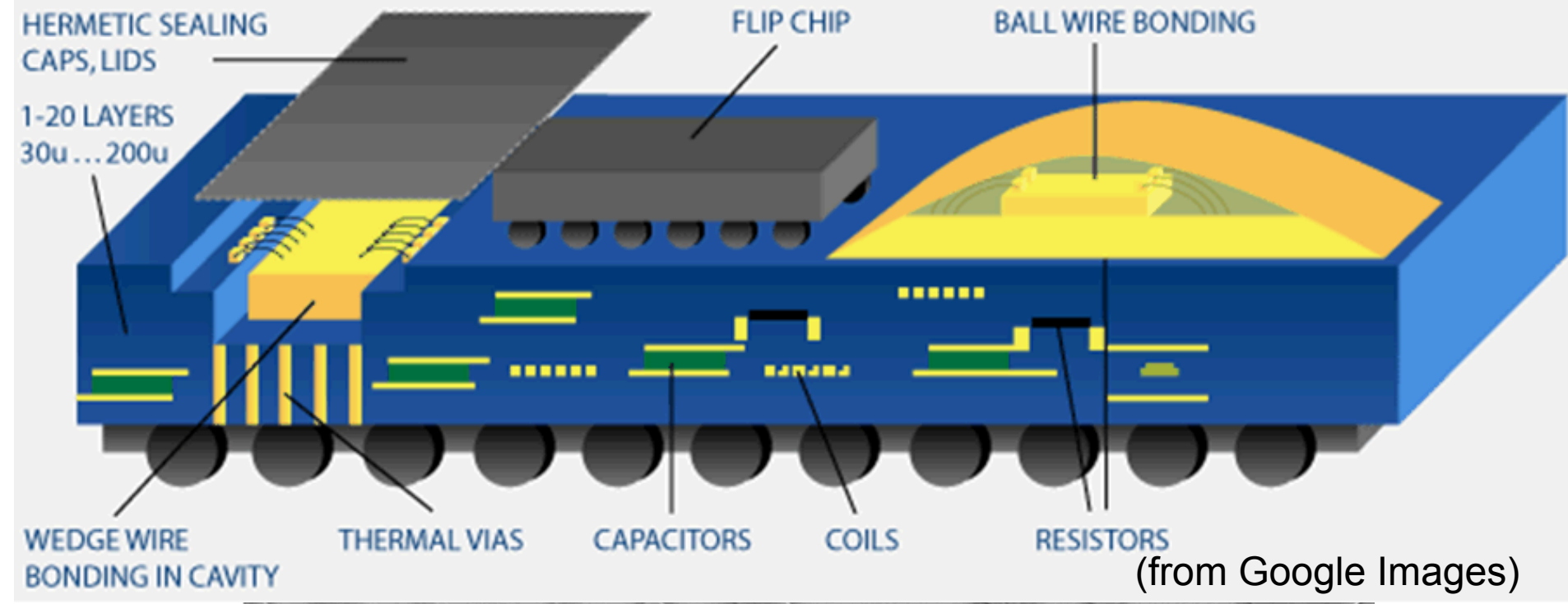
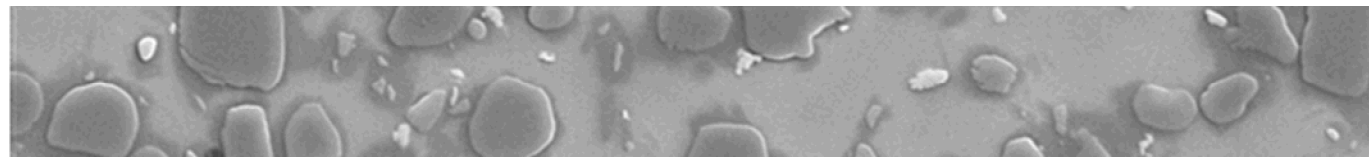
Low/High Temp. Co-fired Ceramics (LTCC/HTCC)

90-96% Alumina: W, Mo, Pt, Au, Ag via High Temperature Sintering
LTCC – Glass/composite ceramics: Cu, Au, Ag via Low Temperature Sintering



Motivation

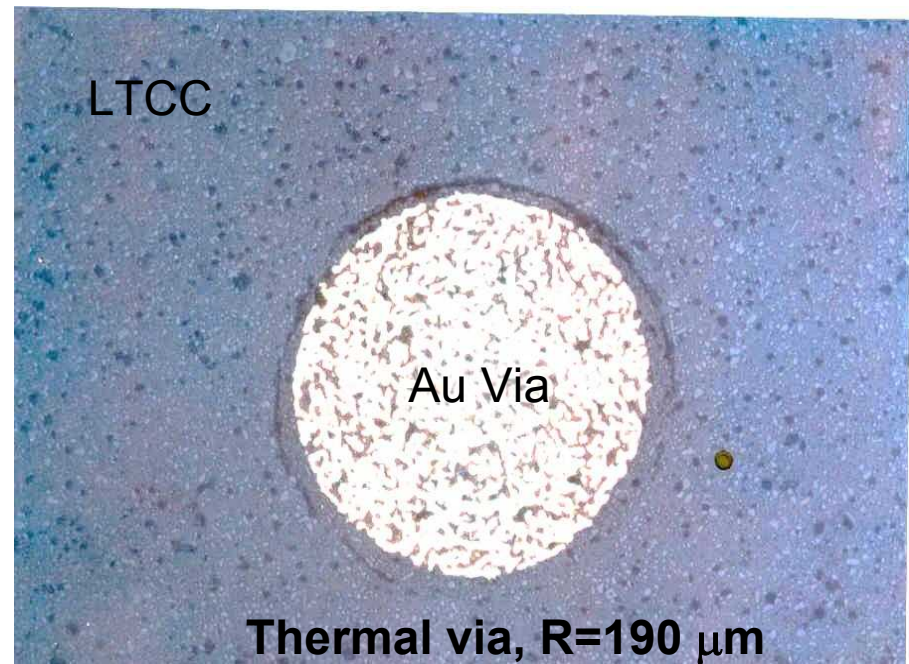
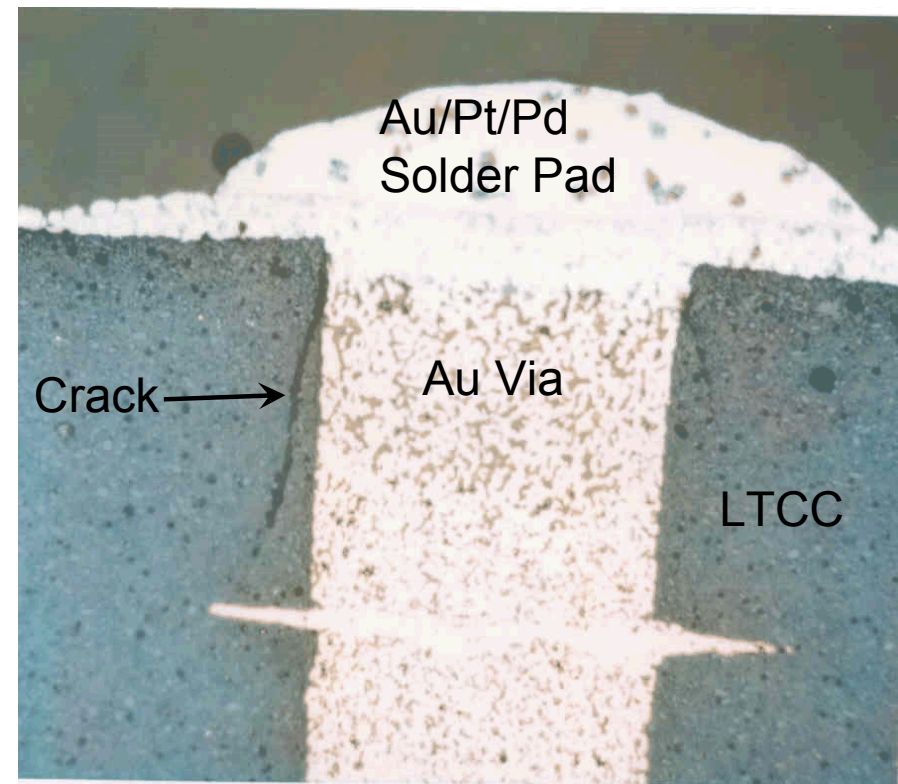
Materials Motivation: Low temp. co-fired ceramic (LTCC) is versatile glass-filled ceramic composite packaging material.



Motivation

Mechanics Motivation: Cylindrical inclusions, such as electrical vias, and metal connector pins are common features in many functional ceramic materials.

Cracking problems are sometimes observed





Outline (Part 1)

- LTCC Work:
 - Experimental Results and Fractographic Observations
 - Interfacial Fracture Mechanics for Cylindrical Inclusions
 - Stress Intensity Factors, and Strain Energy Release Rates
 - Interfacial Fracture Energy Based on Crack Kinking Arguments, & Conclusions



Outline (Part 2)

- HTCC Work

Implantable Medical Devices

Experimental Work

Mechanical Testing for Reliability

Test Vehicles and Approach

Results

Iterative Materials Processing and Testing

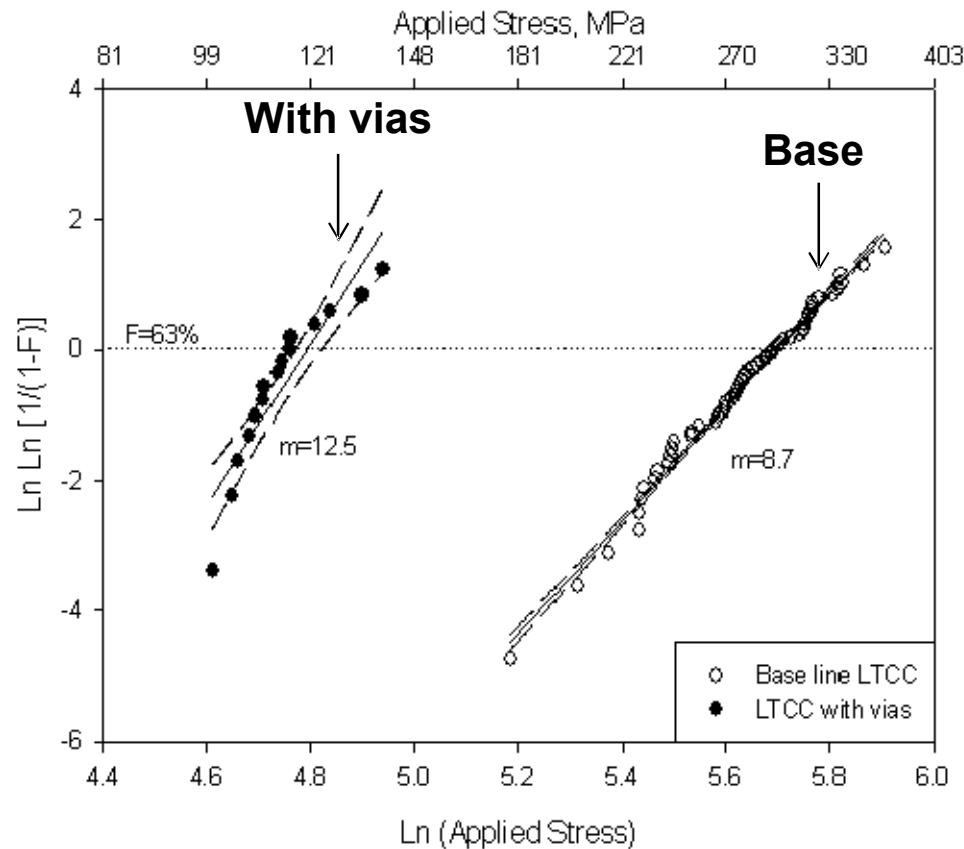
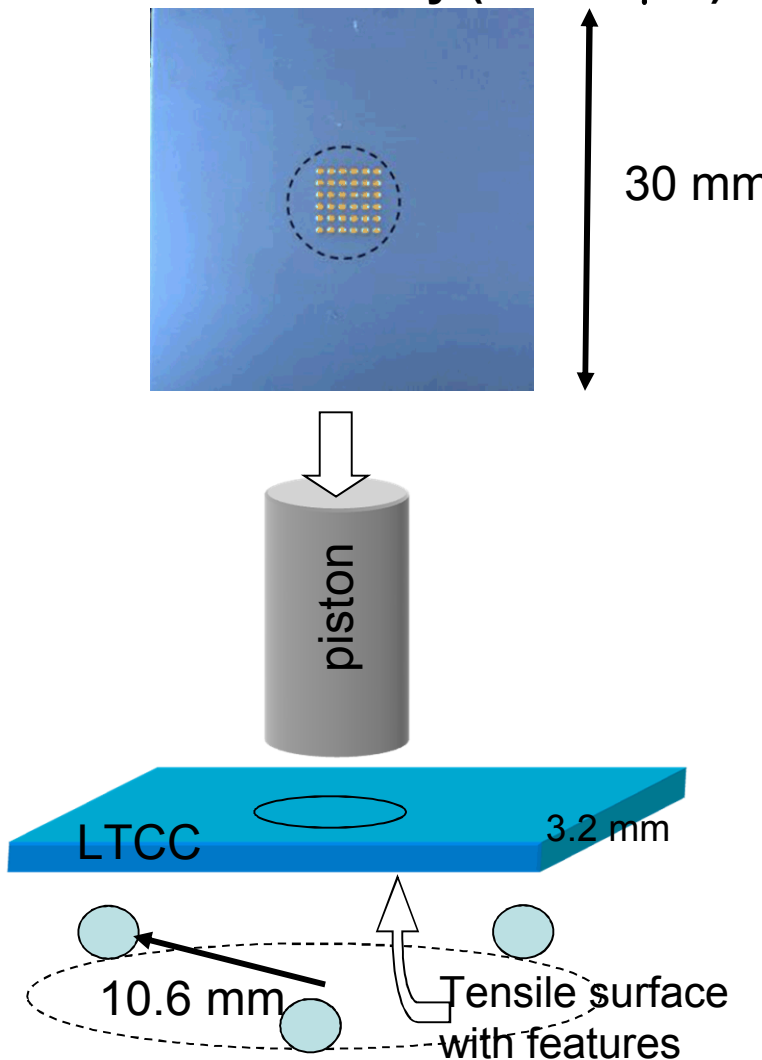
- Phase I, II, and III

Strength, Stresses and Failure Modes

Conclusions

Test Samples and Results

Piston on Ring Strength Tests on a 6x6 via Array ($R=190 \mu\text{m}$)



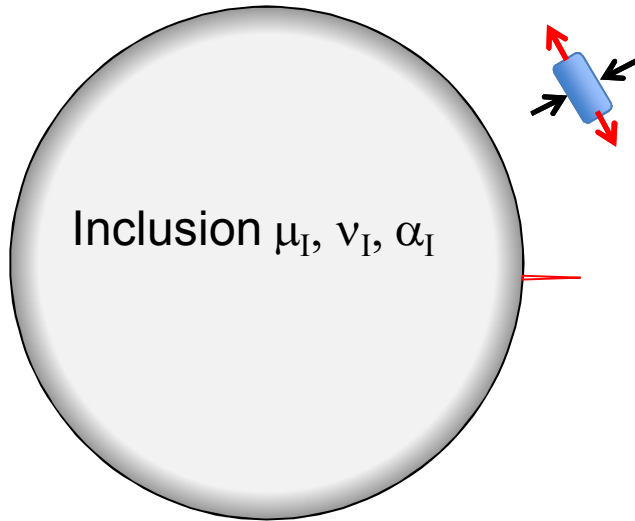
Presence of vias leads to a ~60% reduction in strength.

Why?



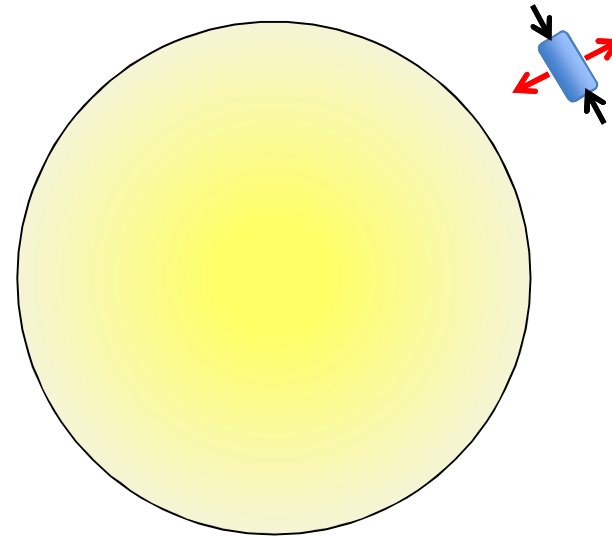
Stresses Around Inclusions

Matrix μ_M, ν_M, α_M



If $\alpha_M > \alpha_I$, circumferential tension in the matrix is generated

This can propagate a radial crack, and lead to lower strength



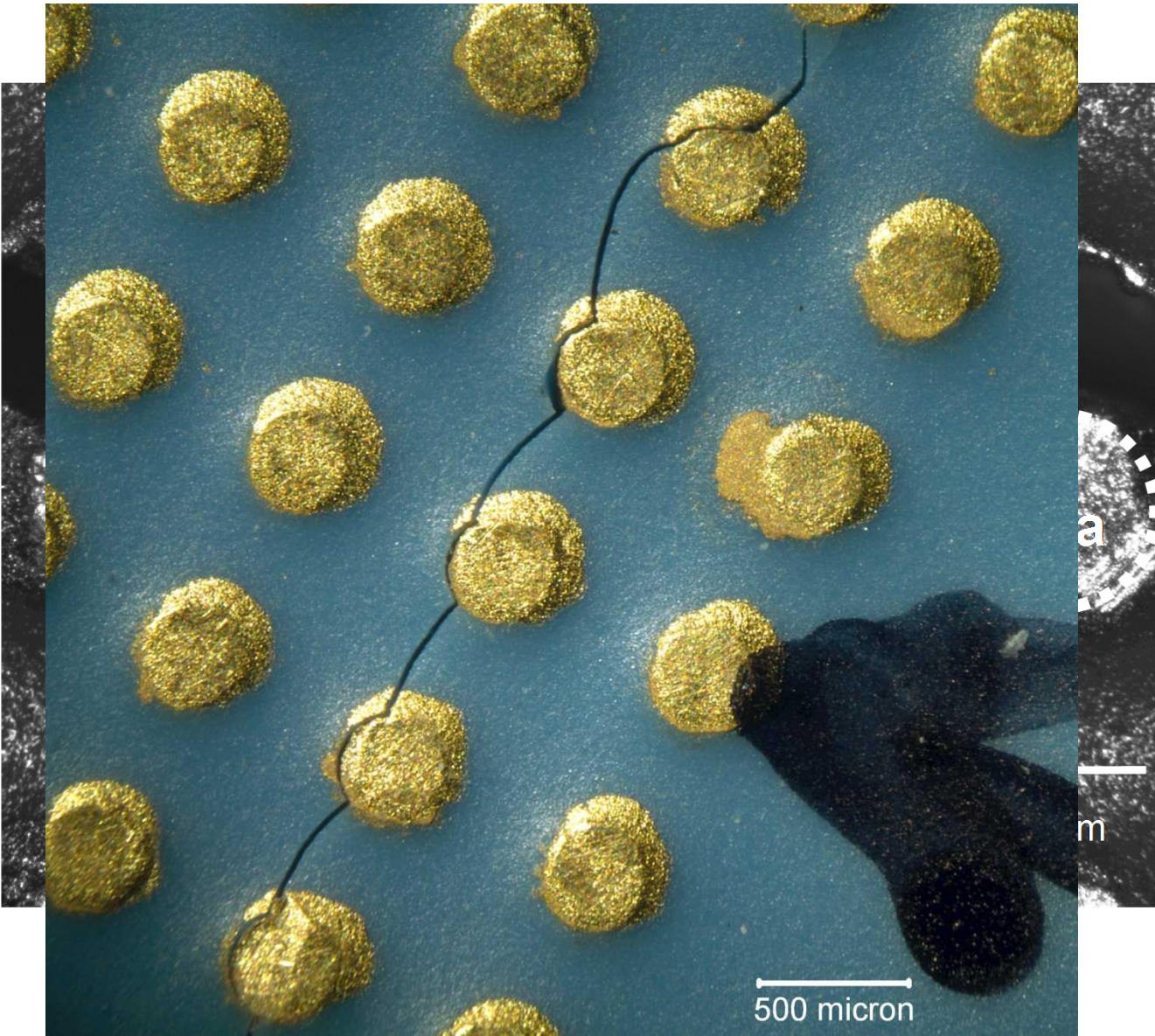
For Au-LTCC:
 α_M (7 ppm) < α_I (16 ppm)

Radial tension

What is the mechanism for strength loss?

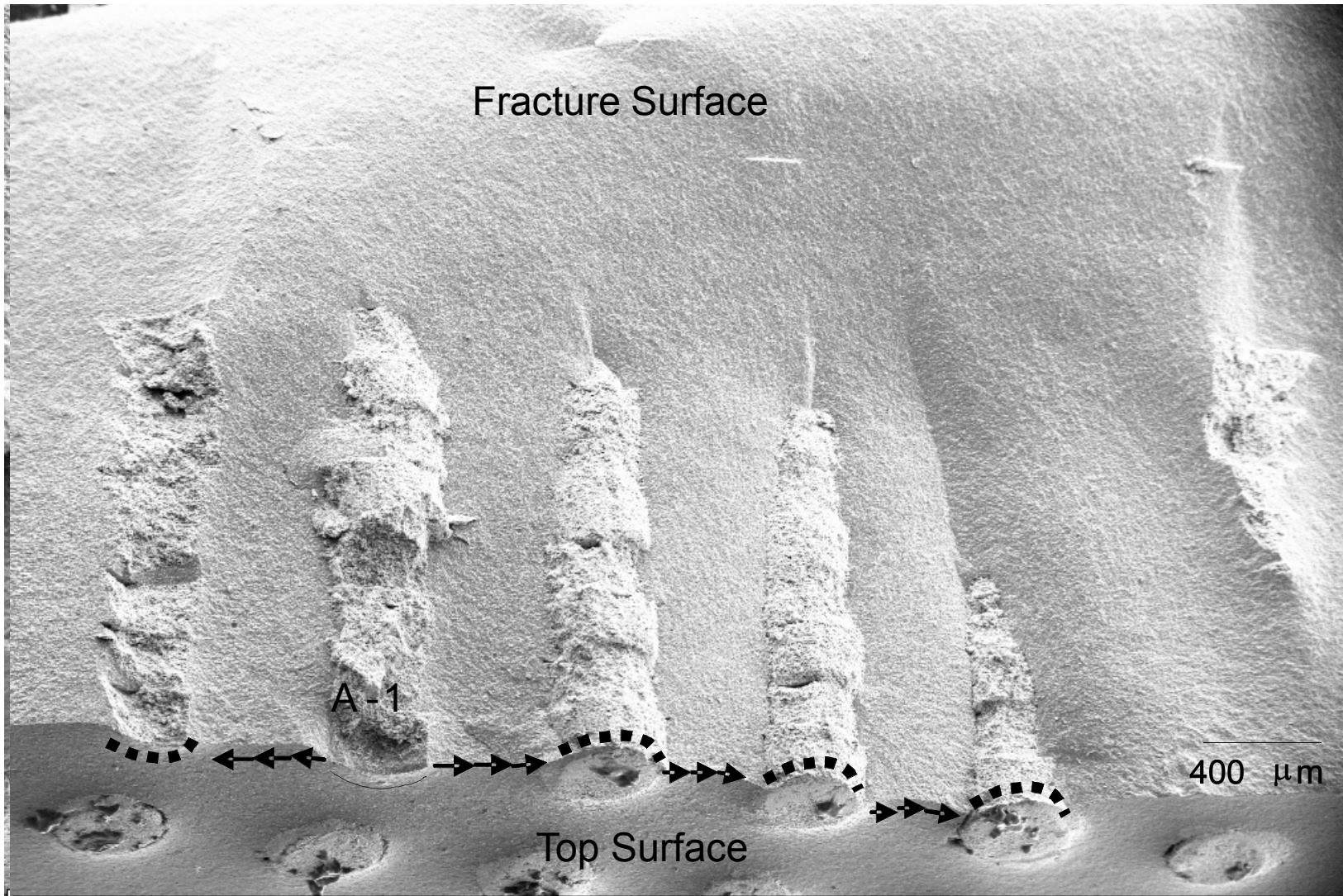


Failure Analysis

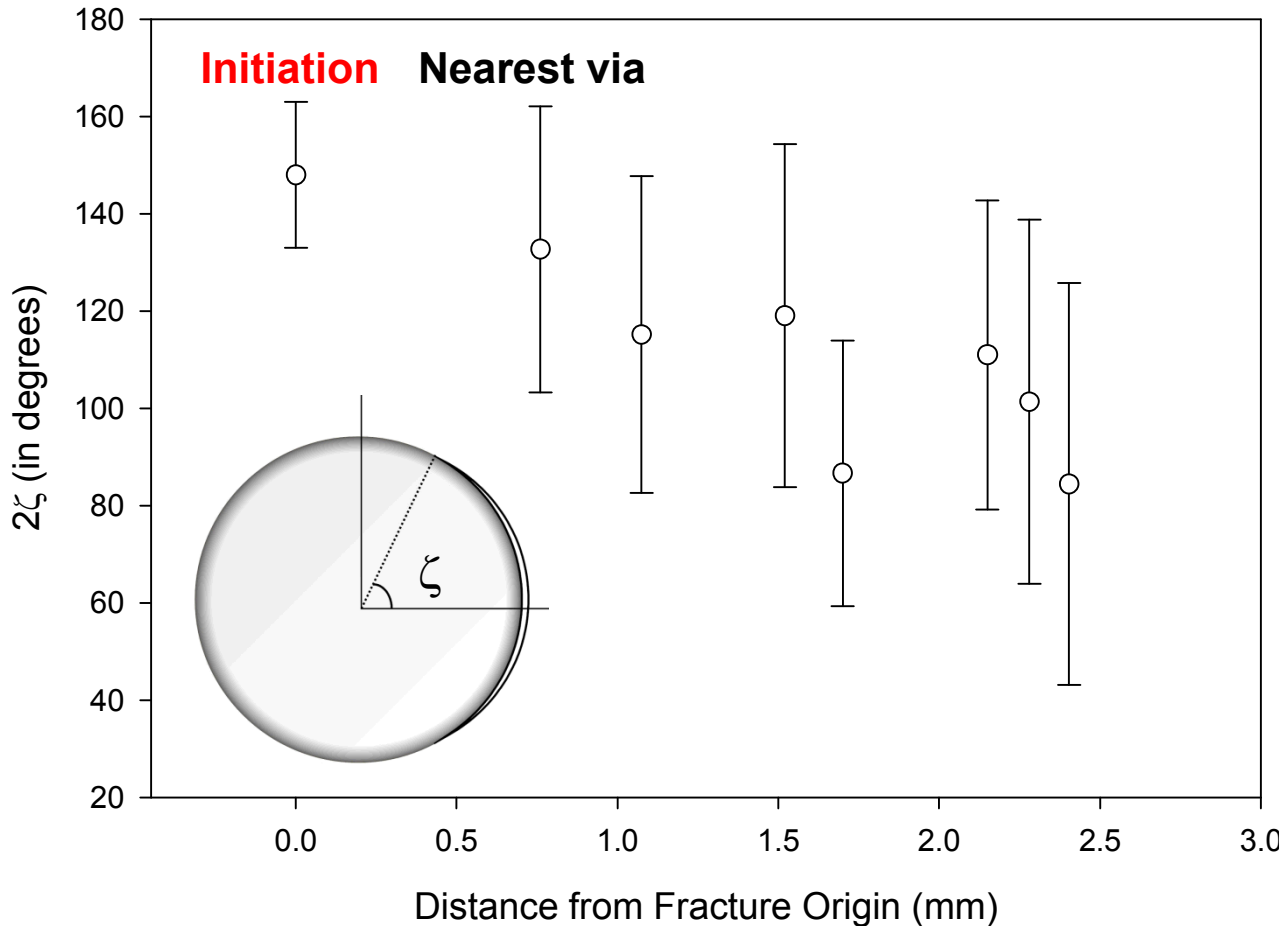




Fracture Surface Analysis

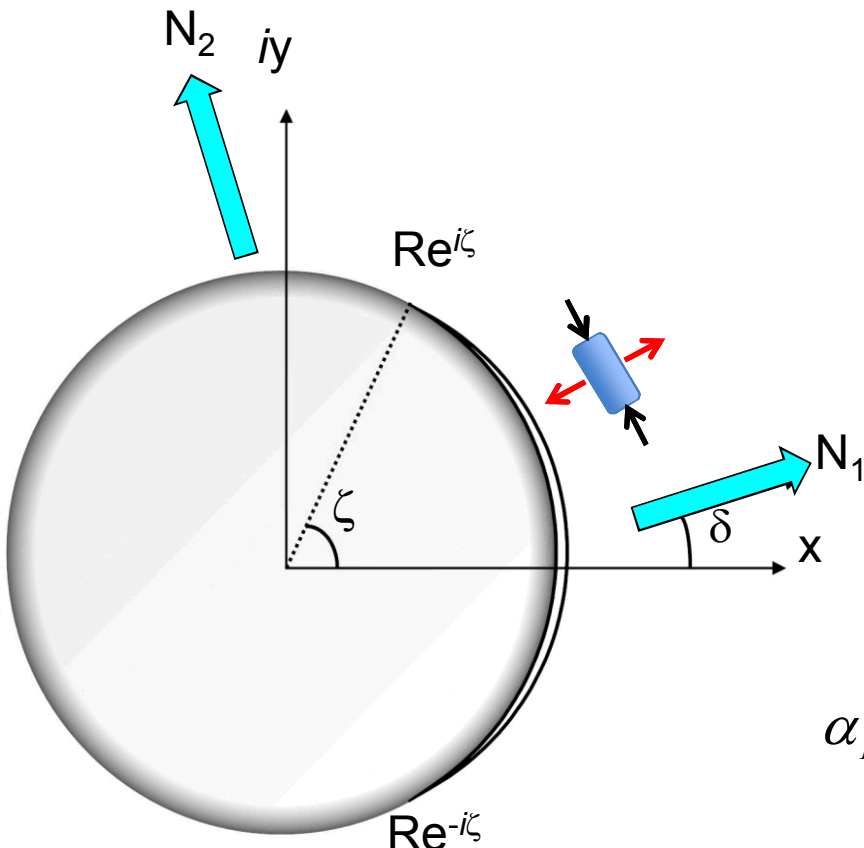


Distribution of Arc Crack Angles



The via causing fracture was identified, and the crack angle at which kinking occurred was measured. $2\zeta=148\pm 15^\circ$.

Interfacial Circumferential Crack Model



Driving Forces:

σ_{rr} = tensile

Biaxial loads, N_1 and N_2

Material, #	E (GPa)	ν	μ (GPa)	α (ppm/ $^{\circ}$ C)
Stress Intensity Factors expressed in terms of Dundur's parameters/oscillatory index				
LTCC, M	116	0.24	47	7
α_{Dundur} fill, μ_I	$\frac{\mu_I (\kappa_M + 1) - \mu_M (\kappa_I + 1)}{\mu_I (\kappa_M + 1) + \mu_M (\kappa_I + 1)}$	$\frac{E_I + E_M}{E_I + E_M}$		
β	$\frac{\mu_I (\kappa_M + 1) - \mu_M (\kappa_I + 1)}{\mu_d_{Dundur} (\kappa_M + 1) + \beta \mu_M (\kappa_I + 1)}$		σ_{th} (MPa)	
γ	$\frac{1}{2\pi} \frac{1 - \beta}{1 + \beta}$	0.01464	0.0046	156

Stress Intensity Factors

K due to Biaxial Loading

$$\mathcal{K}_L = \left(\overline{b}_1 - \overline{b}_2 e^{i\zeta} \right) \sqrt{\pi R \sin \zeta} (1 - 2i\gamma) e^{-\gamma\zeta} e^{i\left(\frac{\zeta}{2} - \gamma \ln(2R \sin \zeta)\right)}$$
$$b_1 = \frac{(1+\alpha)(N_1+N_2) - (1-\alpha^2)(N_1-N_2)(0.25+\gamma^2)\sin^2\zeta \cos 2\delta}{(3+\alpha)(1-\beta) - (1-\alpha)(1+\beta)e^{-2\gamma\zeta}(\cos \zeta + 2\gamma \sin \zeta)} + i \frac{(1+\alpha)(N_1-N_2)(0.25+\gamma^2)\sin^2\zeta \sin 2\delta}{(1-\beta) + (1+\beta)e^{-2\gamma\zeta}(\cos \zeta + 2\gamma \sin \zeta)}$$
$$b_2 = -\frac{1}{2} \frac{(1+\alpha)}{(1+\beta)} (N_1 - N_2) e^{2\gamma\zeta} e^{2\alpha\delta}$$

K due to thermal expansion mismatch

$$\mathcal{K}_{th} = F_0 \sigma_{th} \sqrt{\pi R \sin \zeta} (1 - \alpha) (1 - 2i\gamma) e^{-\gamma\zeta} e^{i\left(\frac{\zeta}{2} - \gamma \ln(2R \sin \zeta)\right)}$$
$$F_0 = f(\alpha, \beta, \gamma) = \frac{2}{(3+\alpha)(1-\beta) - (1-\alpha)(1+\beta)e^{-2\gamma\zeta}(\cos \zeta + 2\gamma \sin \zeta)}$$

$$\sigma_{th} = -\frac{4\mu_2}{1+\kappa_2} (\alpha'_M - \alpha'_I) \Delta T \text{ where } \alpha'_j = \alpha_j \text{ [for plane stress]; or } = (1+\nu_j) \alpha_j \text{ [for plane strain]}$$



Strain Energy Release Rate

$$\mathcal{K}_{Net} = K_1 + iK_2$$

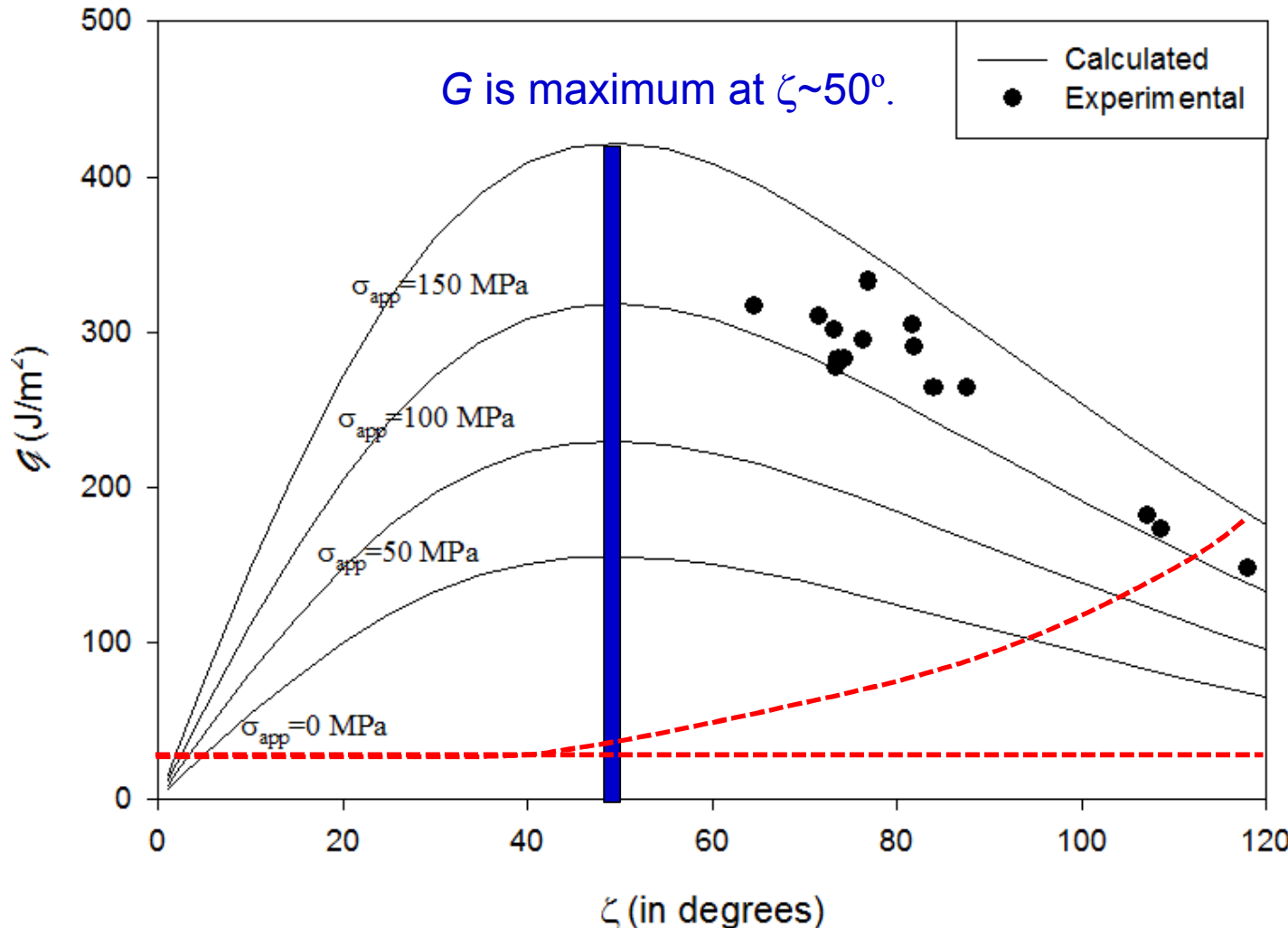
$$K_1 = F_1 \sqrt{\pi R \sin \zeta} (\cos \psi + 2\gamma \sin \psi) e^{-\gamma \zeta}$$

$$K_2 = F_1 \sqrt{\pi R \sin \zeta} (\sin \psi - 2\gamma \cos \psi) e^{-\gamma \zeta}$$

$$F_1 = F_0 \left(\sigma_{app} + \sigma_{th} + \alpha [\sigma_{app} - \sigma_{th}] \right); \psi = \frac{\zeta}{2} + \gamma \ln(2R \sin \zeta)$$

$$G = \frac{\mathcal{K}_{Net} \overline{\mathcal{K}_{Net}}}{4 \cosh^2 \pi \gamma} \left[\frac{1}{\mu_1 (1 + \nu_1)} + \frac{1}{\mu_2 (1 + \nu_2)} \right]$$

G as function of Crack Length (ζ)

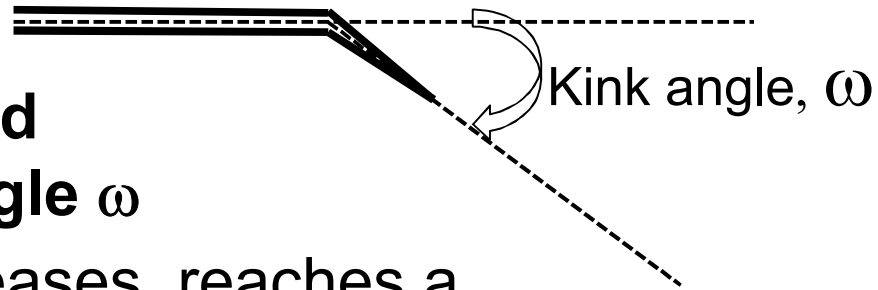


Crack kinking out of interface (into the matrix) occurs on the decreasing portion of G-curve.

Crack Kinking out of Interface

$$\frac{G_{interface}}{G_{max,\omega}} > 1$$

(He et al. J. Am. Ceram Soc. 74, (1991))



- where $G_{max,\omega}$ is the maximized energy release rate at kink angle ω

- with increasing ζ , $G_{interface}$ increases, reaches a maximum, and then decreases.

- At some ζ , $G_{interface} = G_{max,\omega}$ and crack transitions to bulk

$$\frac{G_{interface}}{G_{max,\omega}} = \frac{\Gamma_{interface}}{\Gamma_{substrate}} \bigg|_{Transition}$$

From He et. al, $\Gamma_i/\Gamma_s \sim 0.6$ (for $\alpha=0$), or ~ 0.8 ($\alpha=-0.5$)

For LTCC-AU system, $\alpha=-0.2$, $\Gamma_s \sim 20$ J/m².

Max. $\Gamma_i \sim 12-16$ J/m² – brittle interface



Conclusions

Failure Mechanism:

Crack initiation along the interface

Crack Propagation along the interface aided by the applied &

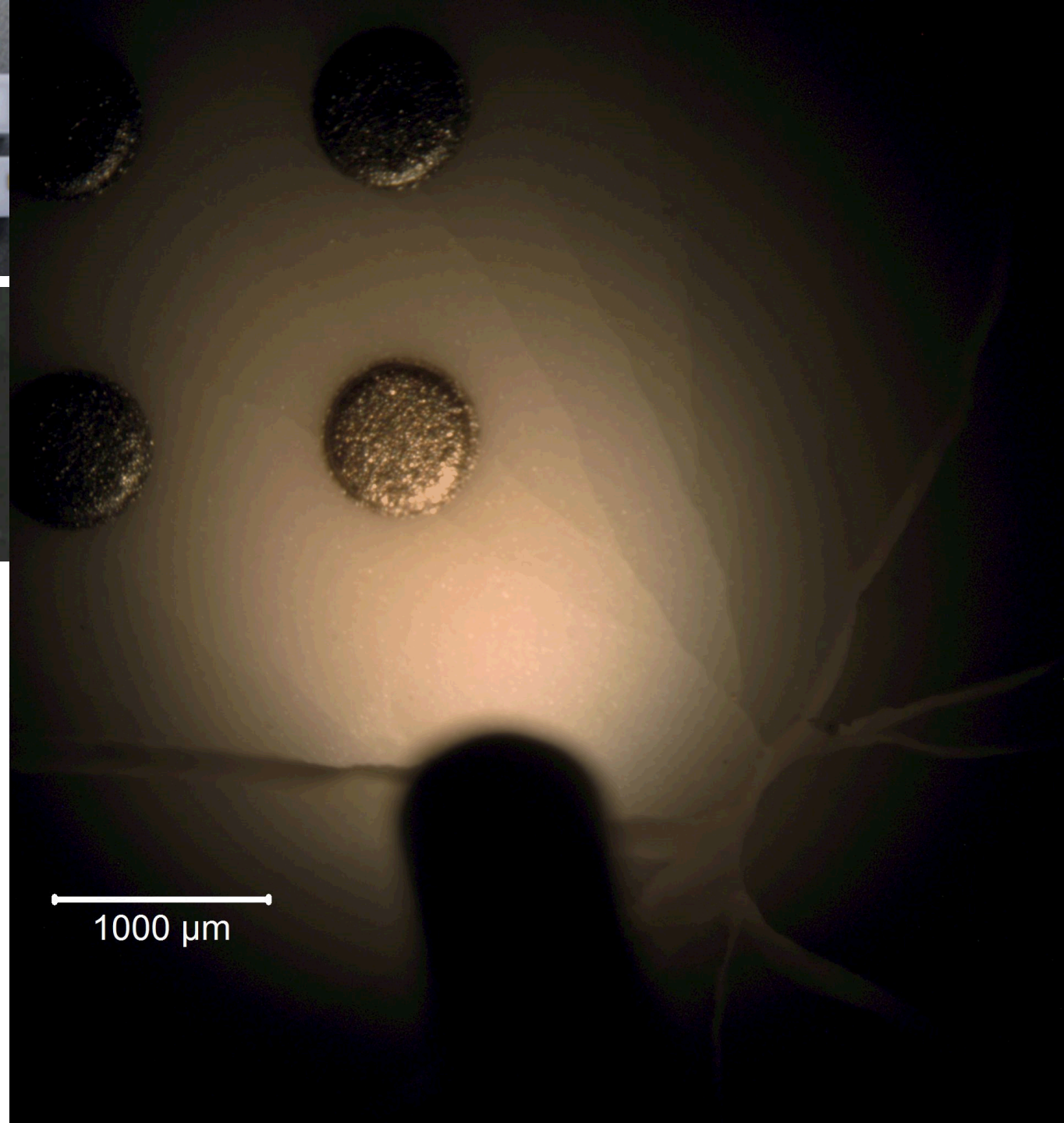
residual stress state

Final fracture after crack kinks into the matrix

Large crack size ($\sim 500 \mu\text{m}$) at failure leads to lower strength

Crack initiation and growth along the interface (and not in the bulk) implies that it is weak, and brittle

Increasing Γ_i , and strength of interface will lead to higher strength



Presentation Outline

Introduction

Implantable Medical Devices

Experimental Work

Mechanical Testing for Reliability

Test Vehicles and Approach

Results

Iterative Materials Processing and Testing

- Phase I, II, and III

Strength, Stresses and Failure Modes

Conclusions

Implantable Medical Devices



Hydrocephalus
Sinus Diseases
Sinus Augmentation
Sleep Disordered Breathing
Cervical Degenerative Disc Disease
Thyroid Conditions



Atrial Fibrillation
Heart Failure
Congenital Heart Disease
Heart Rhythm Disorders
Angina*
Coronary Artery Disease
Heart Valve Disease



Scoliosis
Spinal Fracture
Lumbar Spinal Stenosis
Degenerative Disc Disease
Pelvic Trauma

Peripheral Vascular Disease*



Parkinson's Disease
Essential Tremor
Dystonia**
Obsessive-Compulsive Disorder**



Otologic Disorders
Meniere's Disease
Aortic Disease
Severe Spasticity associated with Multiple Sclerosis, Cerebral Palsy, Stroke and Spinal Cord and Brain Injuries

Chronic Pain
Nausea and Vomiting associated with Gastroparesis**
Diabetes
Overactive Bladder and Urinary Retention
Fecal Incontinence

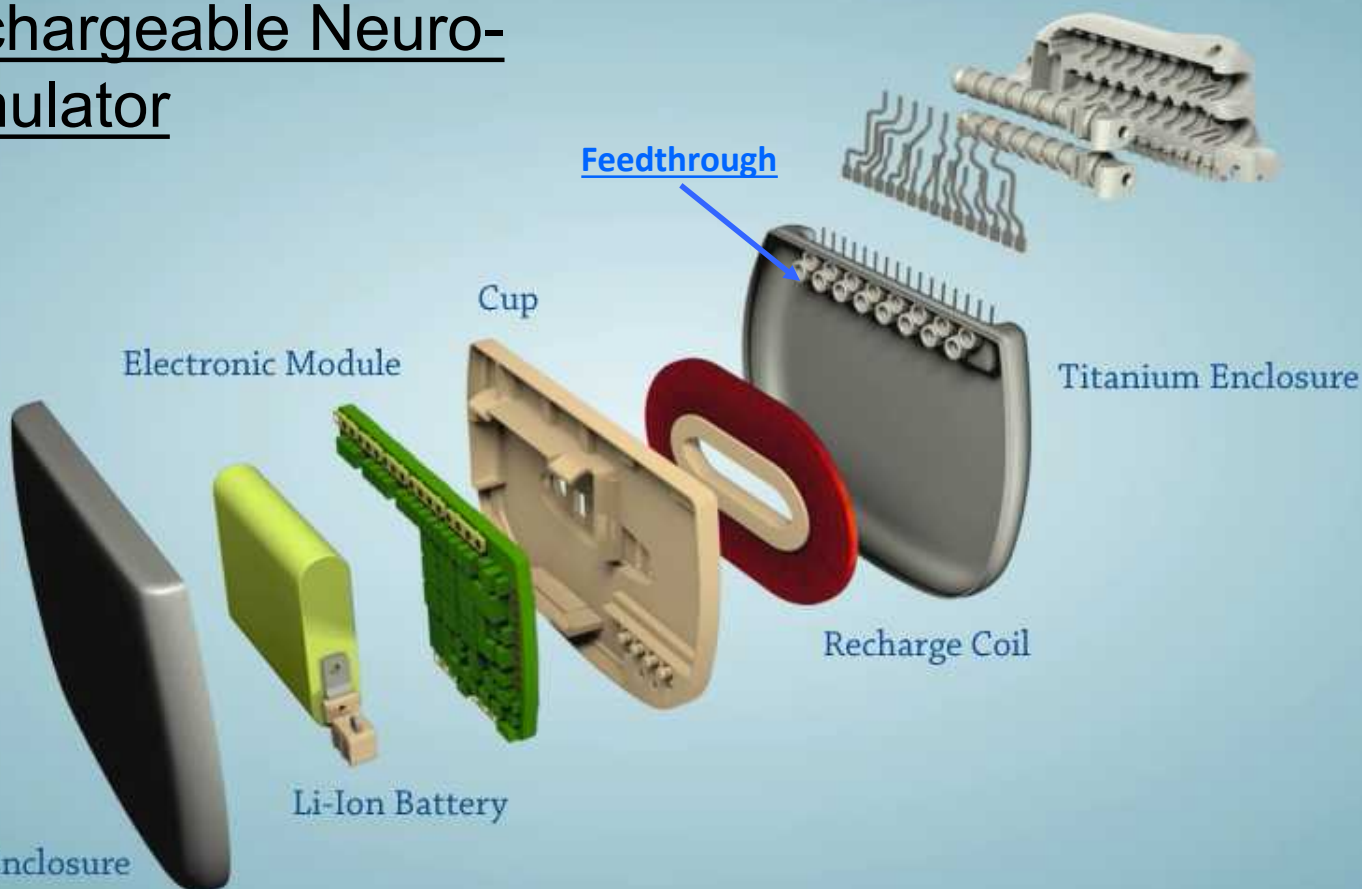
~70 B /per annum

* Not approved for commercial distribution in the United States

** Humanitarian Device in the United States – the effectiveness for this use has not been demonstrated

Implantable Medical Devices

Rechargeable Neuro-stimulator

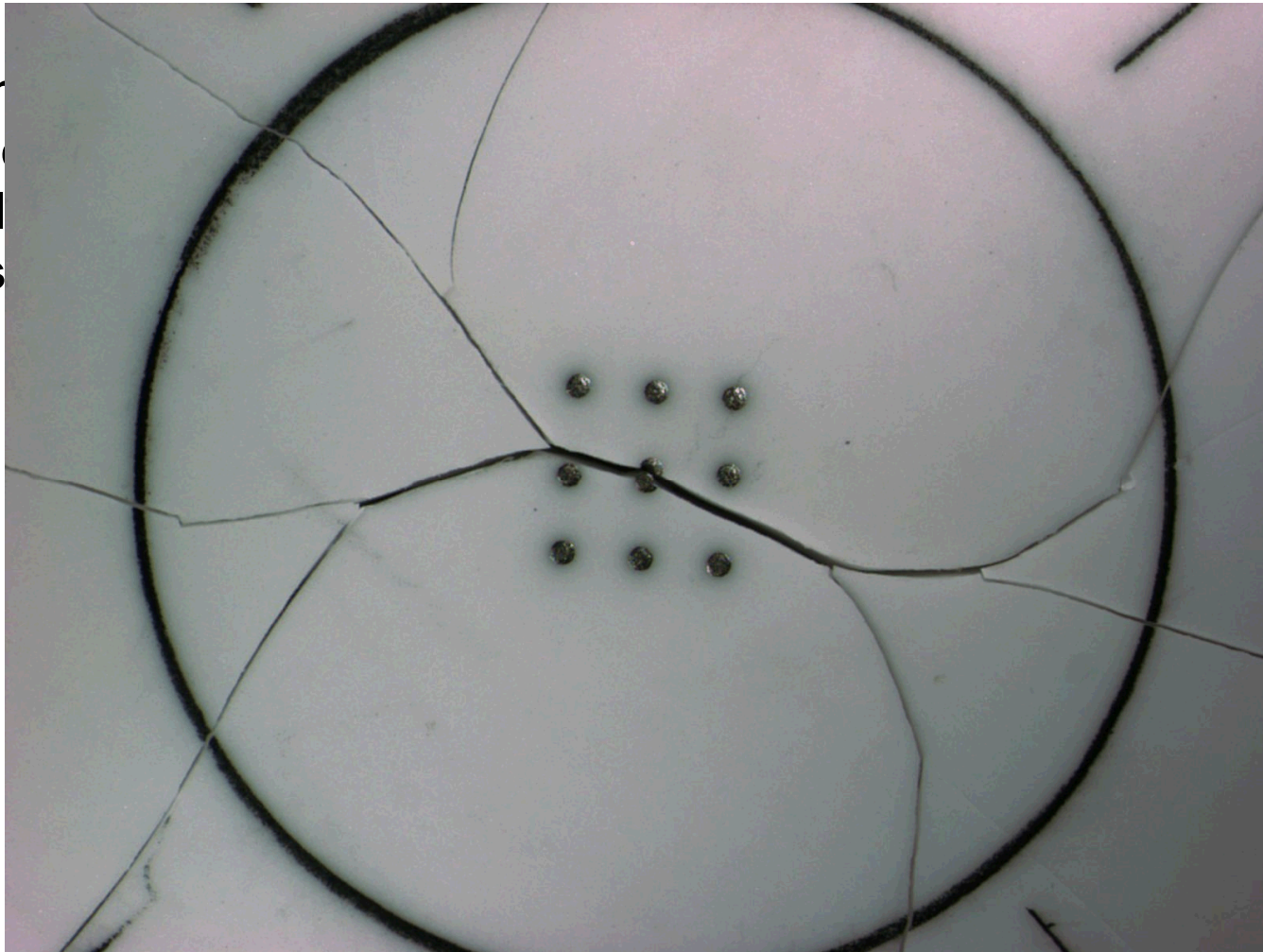


Hermetic Feedthroughs for Medical Devices

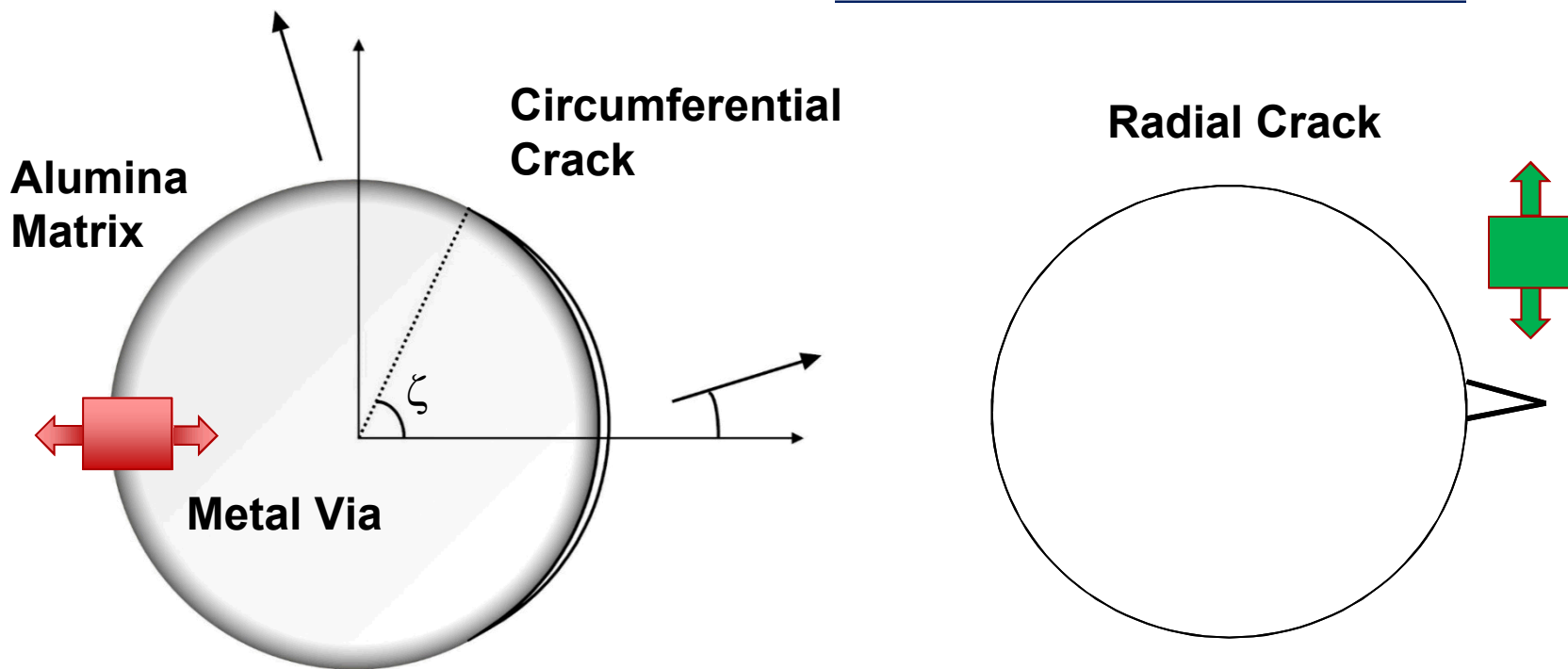
Alumina - High Temperature Co-fired Ceramic (HTCC)

Physical and electrical characteristics for high-reliability applications:

- Mechanical strength
- High temperature stability
- Ease of processing
- Passivation
- ...



Stress State Around a Via Impacts Strength



Local residual stress – Due to thermal and elastic mismatches, modified by plasticity of via material

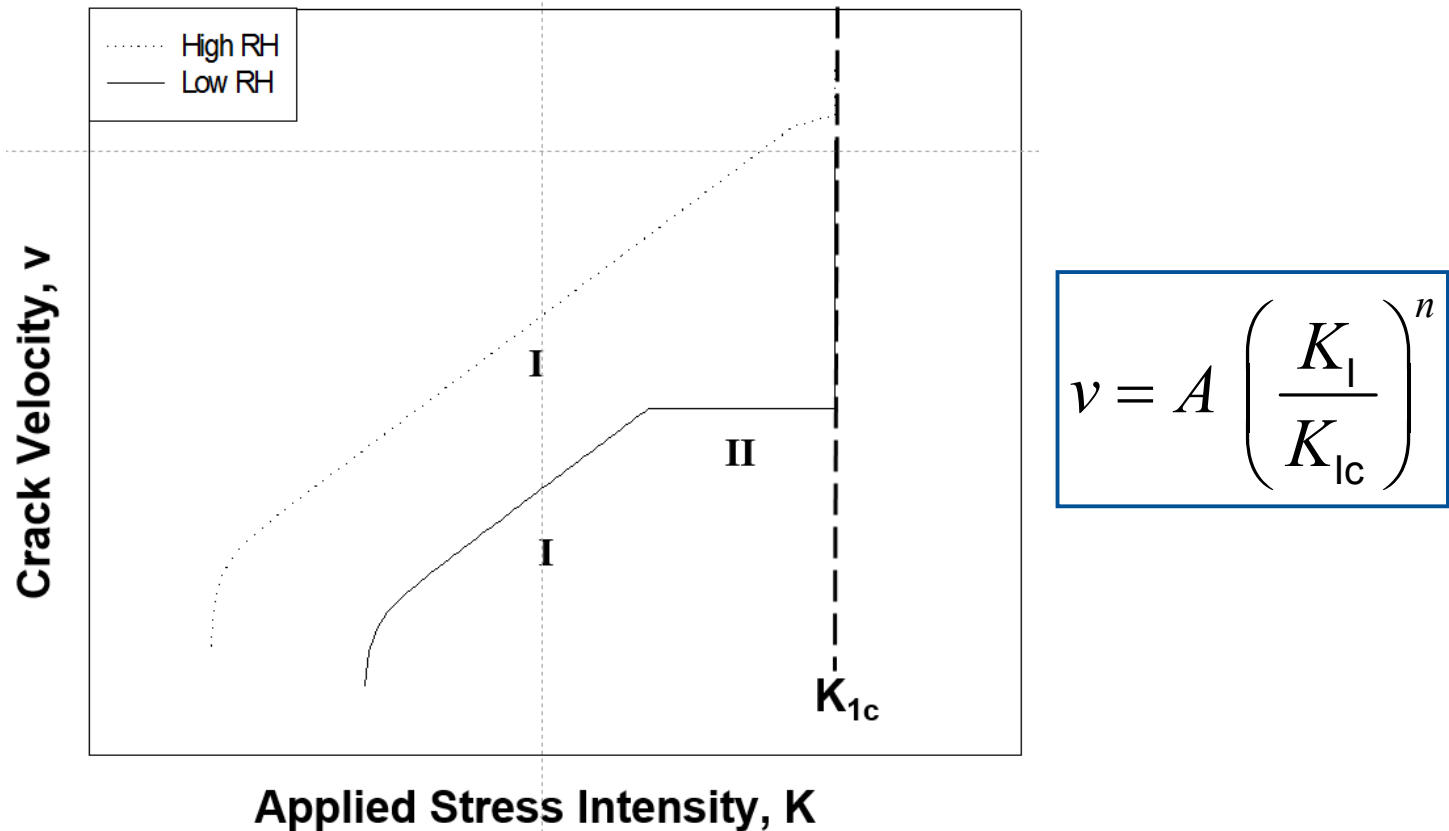
Higher thermal expansion via

~Similar expansion via + plasticity

Externally applied stresses – Thermal transients, & due to brazing/welding of material

Combination of these stresses can lead to Sub-Critical Crack Growth (SCG): can cause leaks, crack growth and failure

Sub-Critical Crack Growth (SCG)

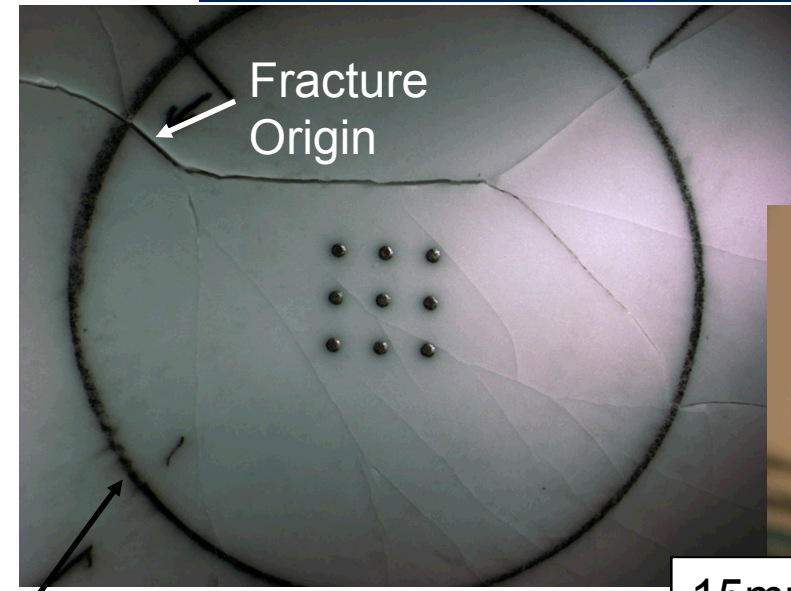


SCG behavior was quantified by conducting strength tests as a function of loading rates (*ASTM C1368: Test method for SCG Parameters*)

Materials with and without vias were strength tested in 20% RH, and in 0.9% saline (simulated body fluid)*

*<https://www.ncbi.nlm.nih.gov/pmc/articles/PMC3683025/>

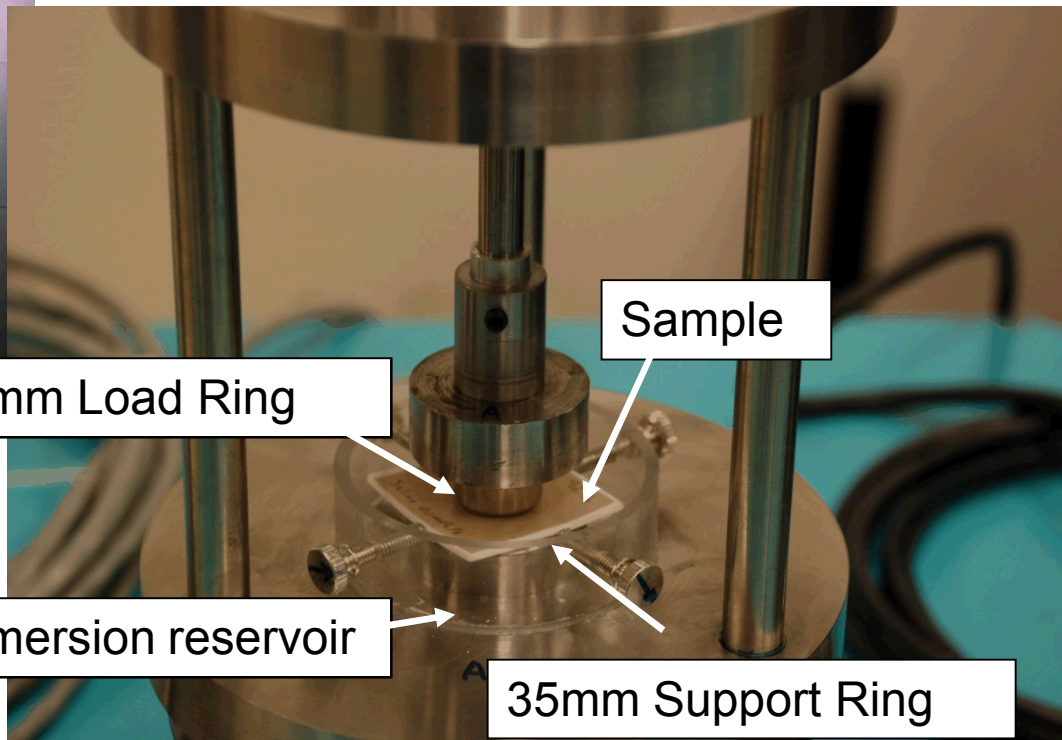
Reliability of Devices



Tensile region
(inside black circle)



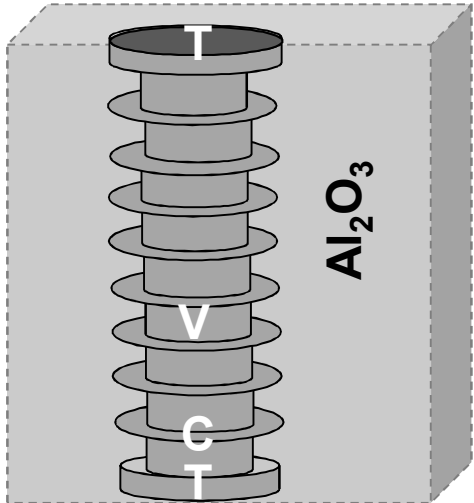
Sample Size: $40\text{mm}^2 \times 2\text{mm}$
Loading rings made of Tefzel material



(ASTM C1368 strength testing)

Via Materials Optimization – Phase I

Phase I



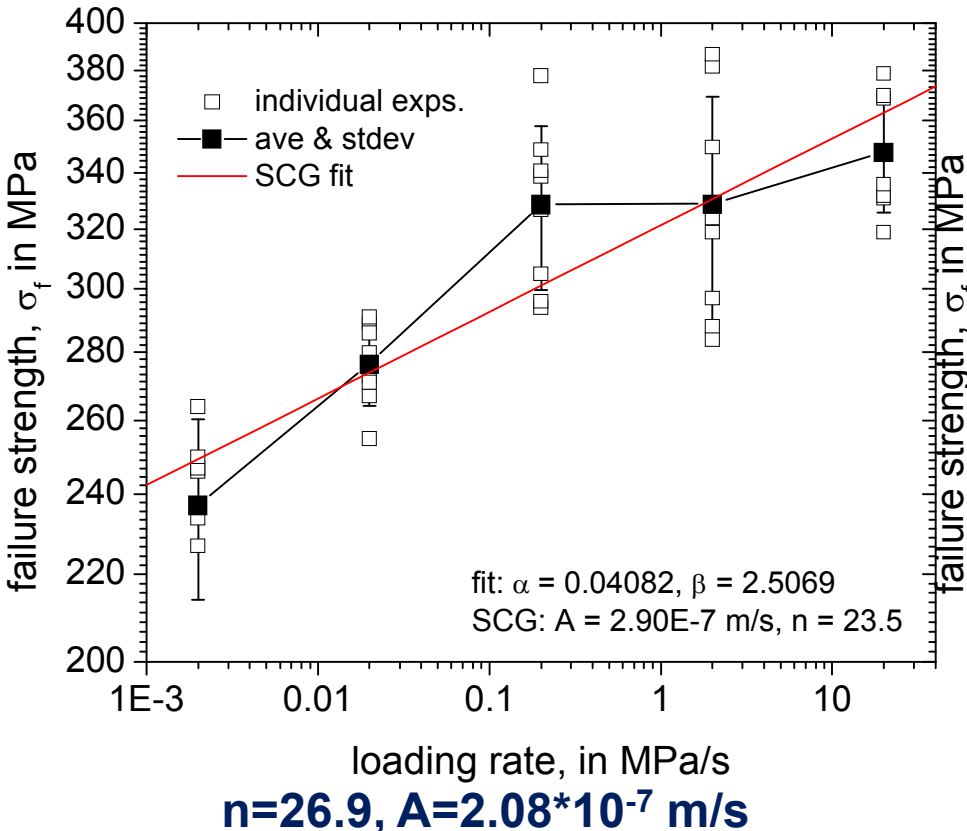
- Standard HTCC cofire process
- Commercial 92% Al_2O_3
- 0.2mm vias, 0.150mm layers
- Fired in Air atmosphere (vs N_2)

Top Pad (T)	100% Pt_f	50 Pt_f / 50% Pt_c	75 Pt_f / 25% Pt_c + 5% Al_2O_3
Base Pad (B)	-	50 Pt_f / 50% Pt_c + 5% Al_2O_3	75 Pt_f / 25% Pt_c + 5% Al_2O_3
Via (V)	Pt + 5% (CaO, SiO_2 , MgO, Al_2O_3)	50 Pt_f / 50% Pt_c + 5% Al_2O_3	75 Pt_f / 25% Pt_c + 5% Al_2O_3
Cover Pads(C)	Pt + 5% Al_2O_3	50 Pt_f / 50% Pt_c + 5% Al_2O_3	75 Pt_f / 25% Pt_c + 5% Al_2O_3

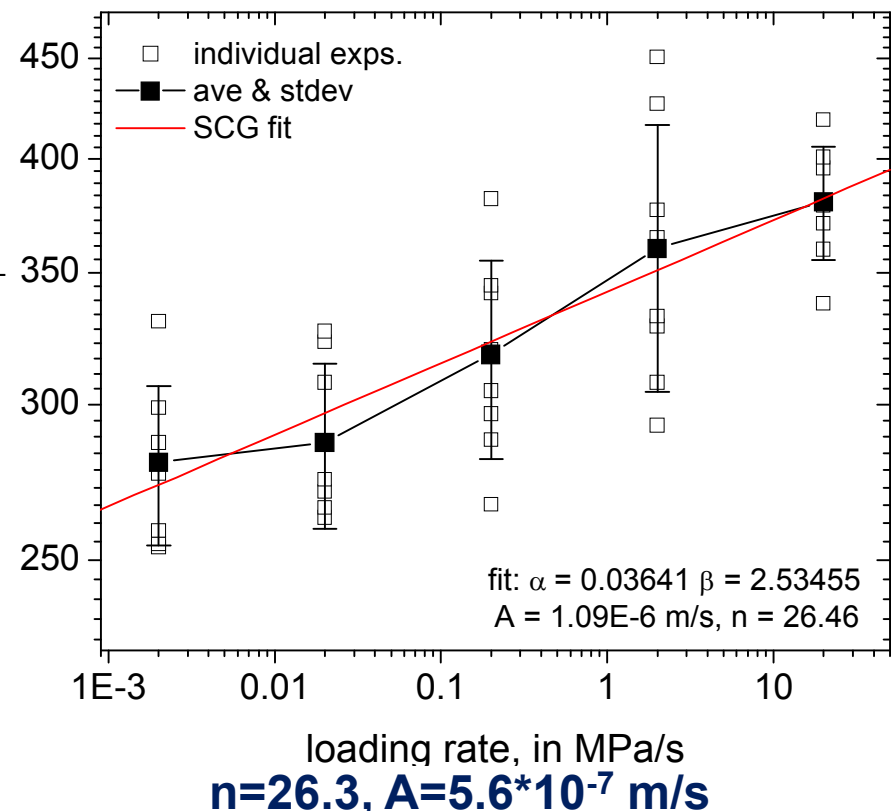
Phase I – 20% RH Air

$$v = A \left(\frac{K_I}{K_{lc}} \right)^n$$

No Vias- Base 92% Alumina



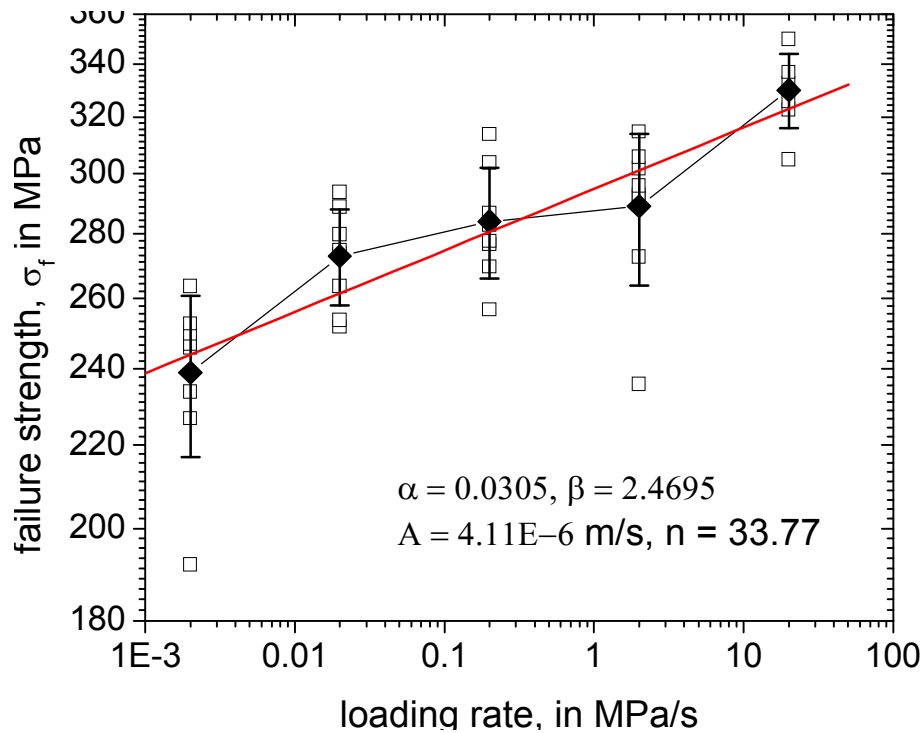
Alumina with Vias



n values ~ those of alumina in literature
Strength Response in air is not affected by vias

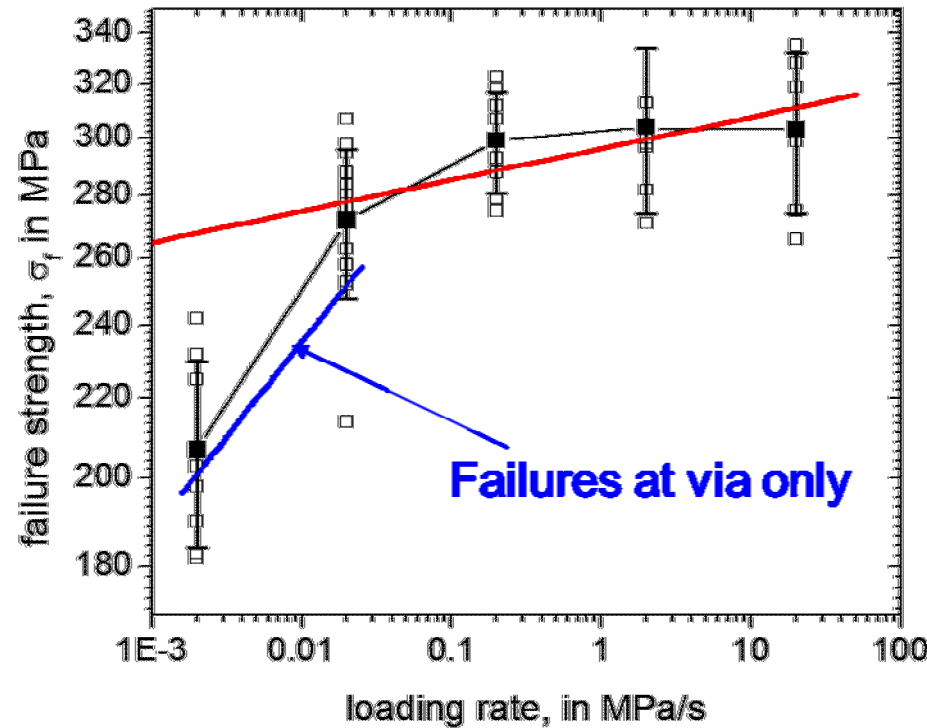
Phase I- Saline Immersion (*in vivo* simulation)

No Vias- Base 92% Alumina



$$n=36.7, A=4.54*10^{-6} \text{ m/s}$$

Alumina with Vias



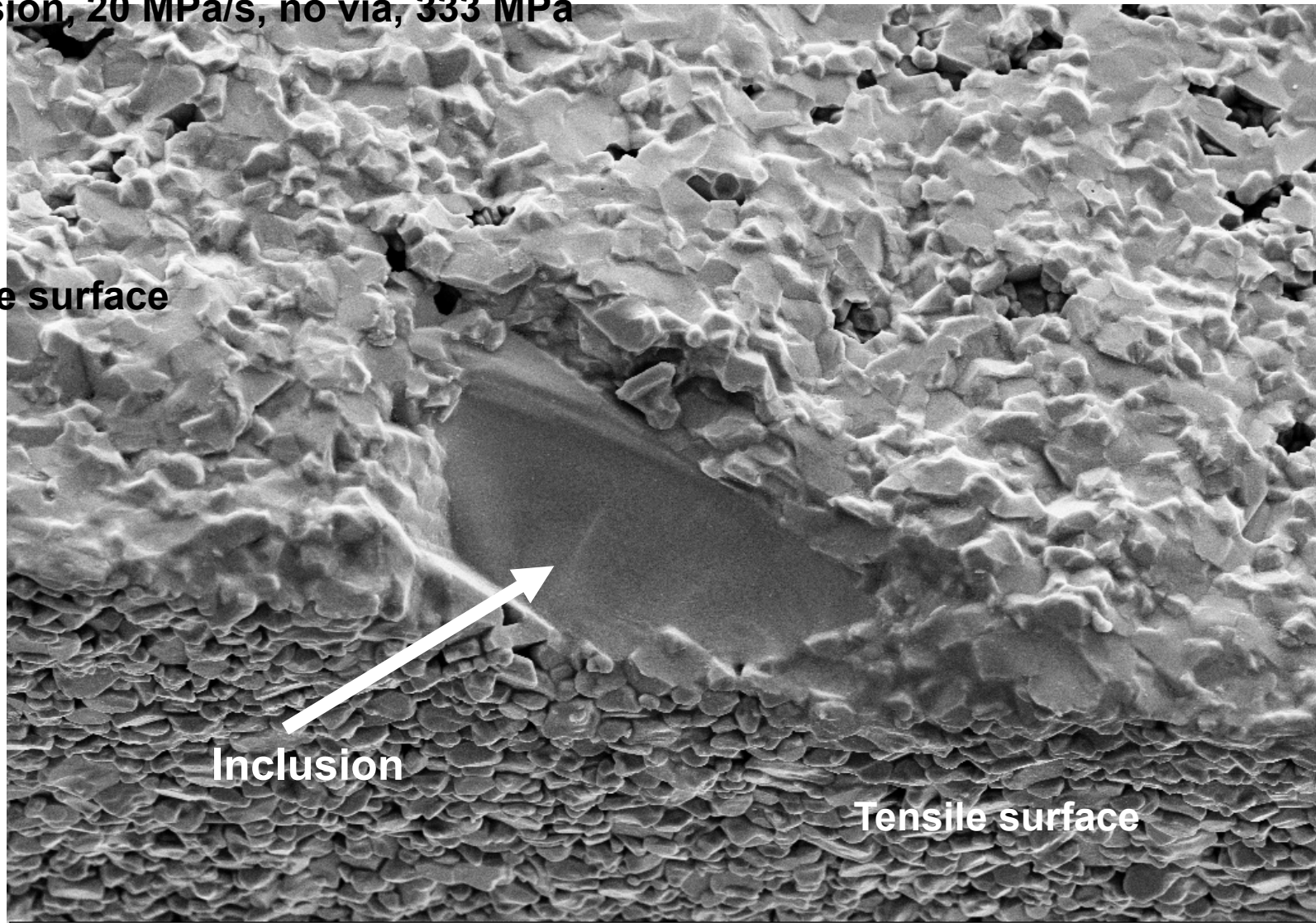
$$n=38.1, A=5.07*10^{-8} \text{ m/s}$$

At Via $n=9.2, A=1.0*10^{-8} \text{ m/s}$

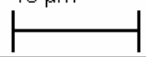
Vulnerability: Slow rates and saline environment

Fractography- Hard Inclusion

Immersion, 20 MPa/s, no via, 333 MPa



10 μ m

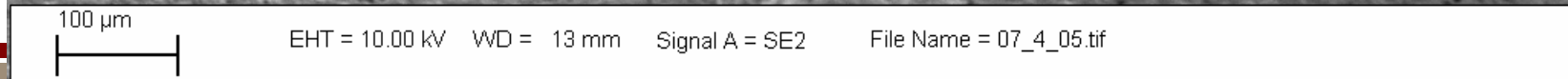
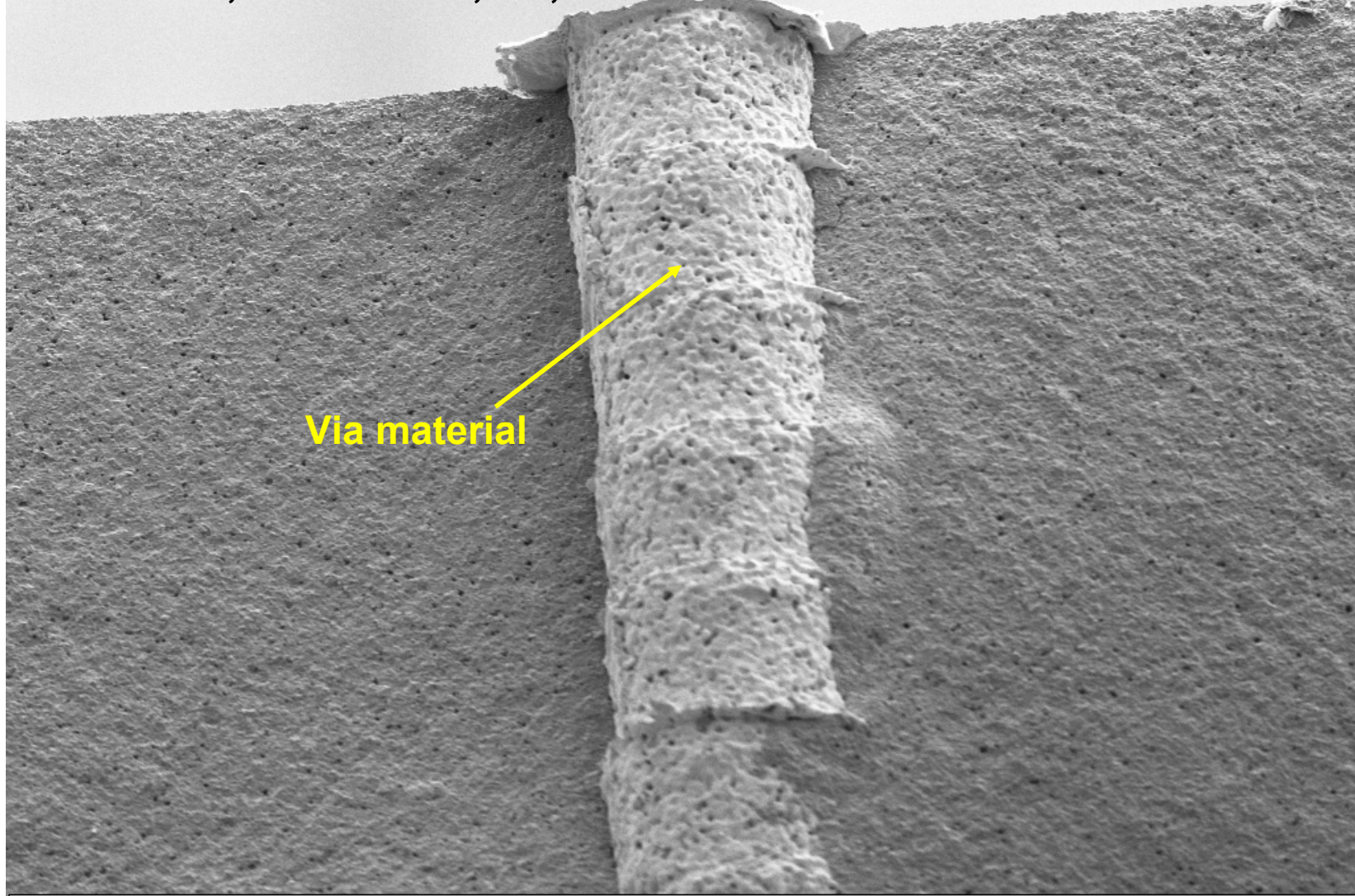


EHT = 10.00 kV WD = 12 mm Signal A = SE2

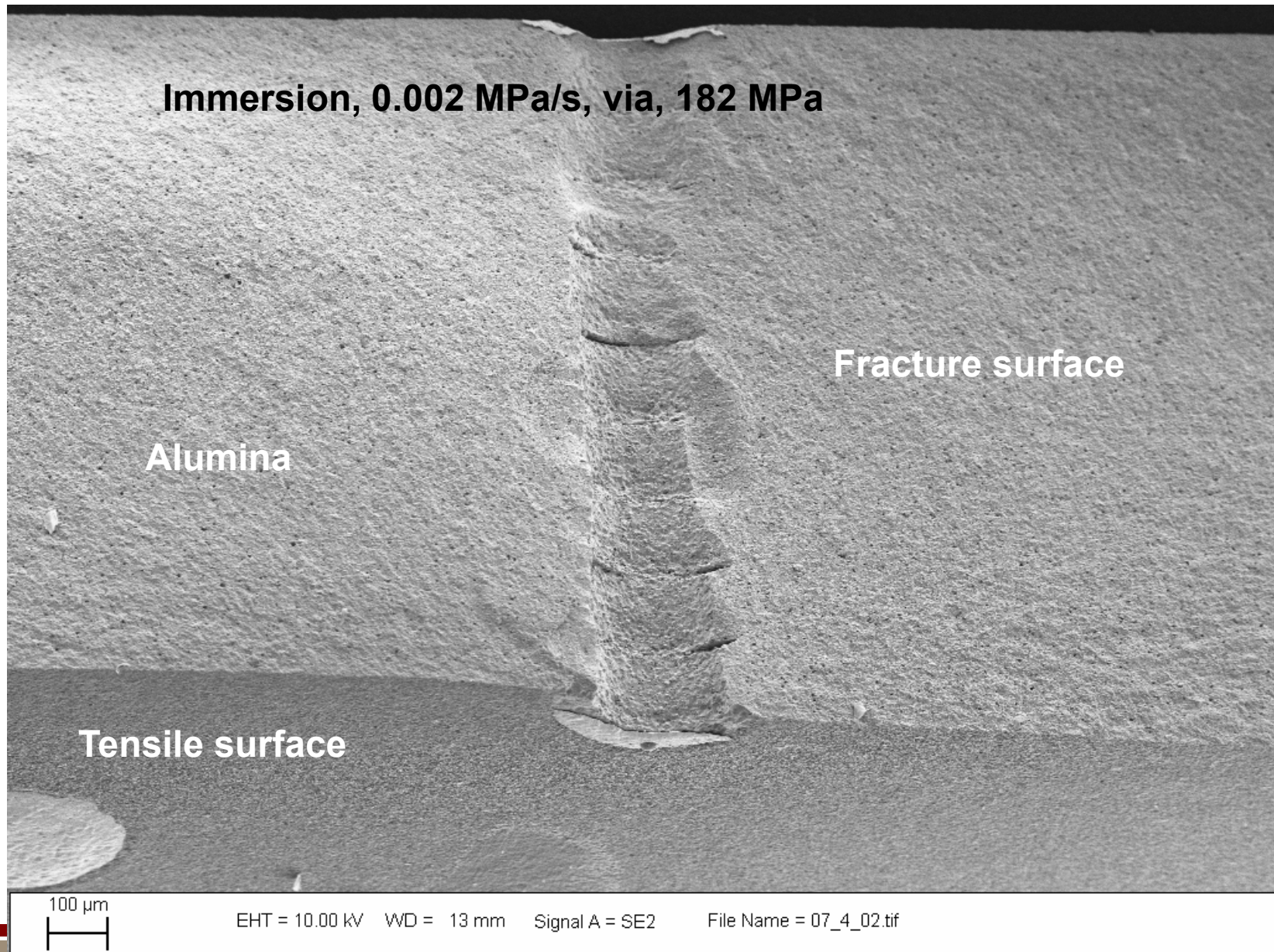
File Name = 04_6_03.tif

Fractography – Via Separation - A

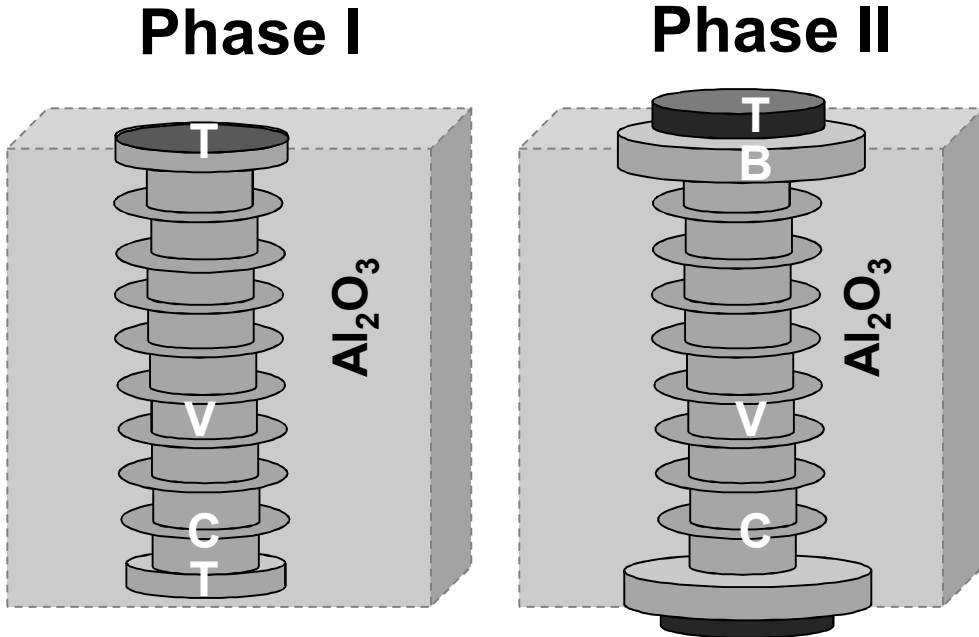
Immersion, 0.002 MPa/s, via, 182 MPa



Fractography – Via Separation - B



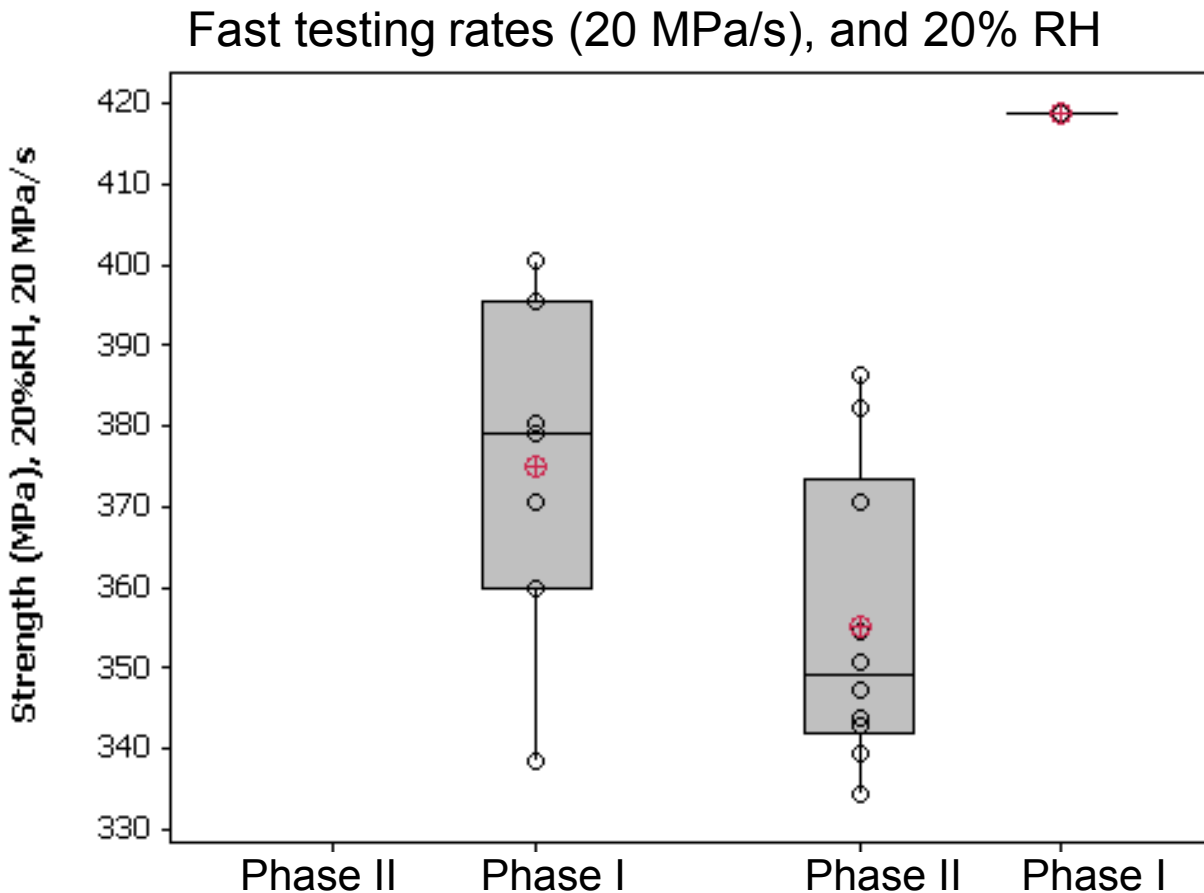
Via Materials Optimization – Phase II



- 50/50 blend of fine/coarse Pt
- Removal of $\text{Ca}/\text{MgO}/\text{SiO}_2$
- Addition of base pad
- Process mods.

Top Pad (T)	100% Pt_f	50 $\text{Pt}_f/50\% \text{Pt}_c$	75 $\text{Pt}_f/25\% \text{Pt}_c + 5\% \text{Al}_2\text{O}_3$
Base Pad (B)	-	50 $\text{Pt}_f/50\% \text{Pt}_c + 5\% \text{Al}_2\text{O}_3$	75 $\text{Pt}_f/25\% \text{Pt}_c + 5\% \text{Al}_2\text{O}_3$
Via (V)	$\text{Pt} + 5\% (\text{CaO}, \text{SiO}_2, \text{MgO}, \text{Al}_2\text{O}_3)$	50 $\text{Pt}_f/50\% \text{Pt}_c + 5\% \text{Al}_2\text{O}_3$	75 $\text{Pt}_f/25\% \text{Pt}_c + 5\% \text{Al}_2\text{O}_3$
Cover Pads(C)	$\text{Pt} + 5\% \text{Al}_2\text{O}_3$	50 $\text{Pt}_f/50\% \text{Pt}_c + 5\% \text{Al}_2\text{O}_3$	75 $\text{Pt}_f/25\% \text{Pt}_c + 5\% \text{Al}_2\text{O}_3$

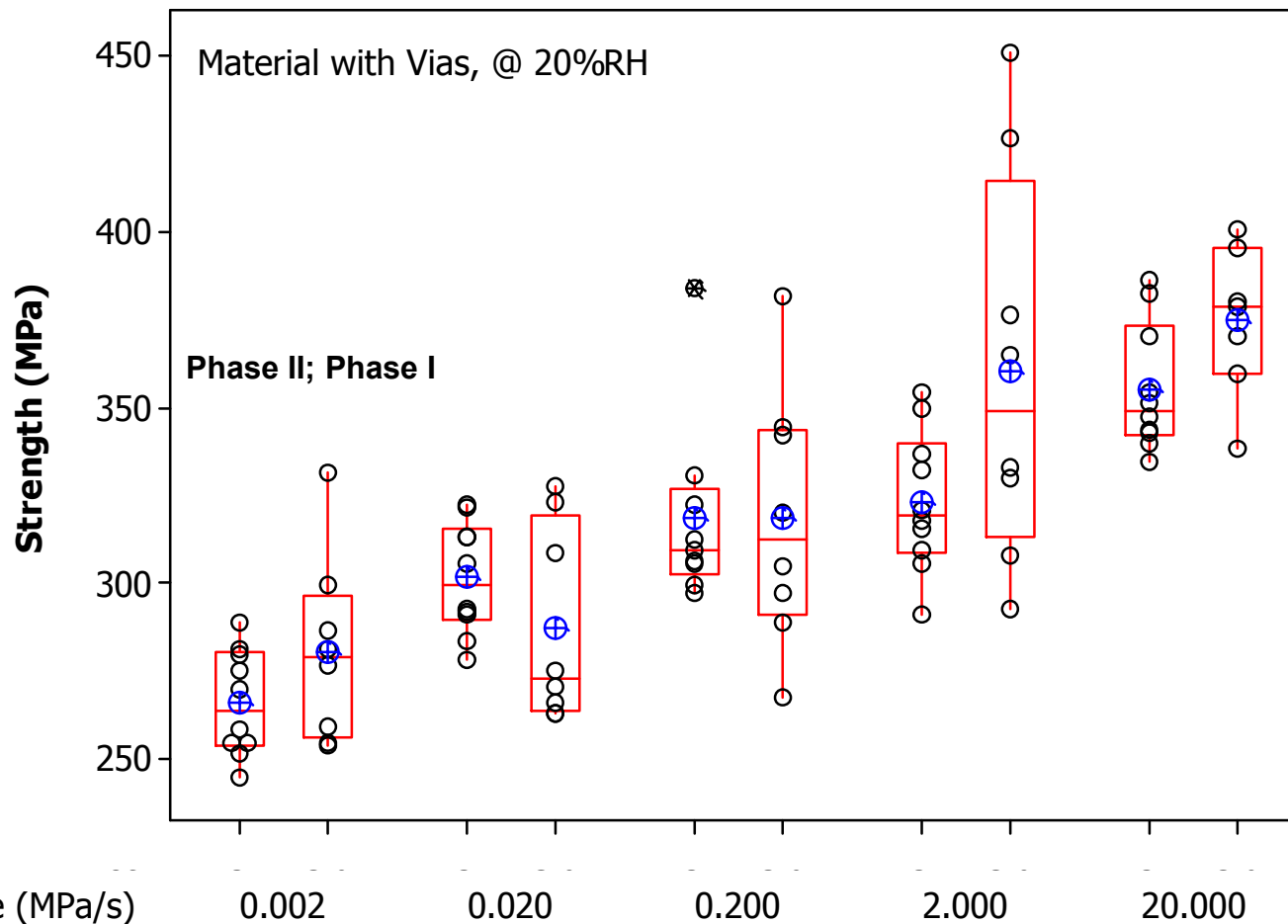
Phase II – 20% RH, Alumina with Via



The new batch of samples have lower mean strength

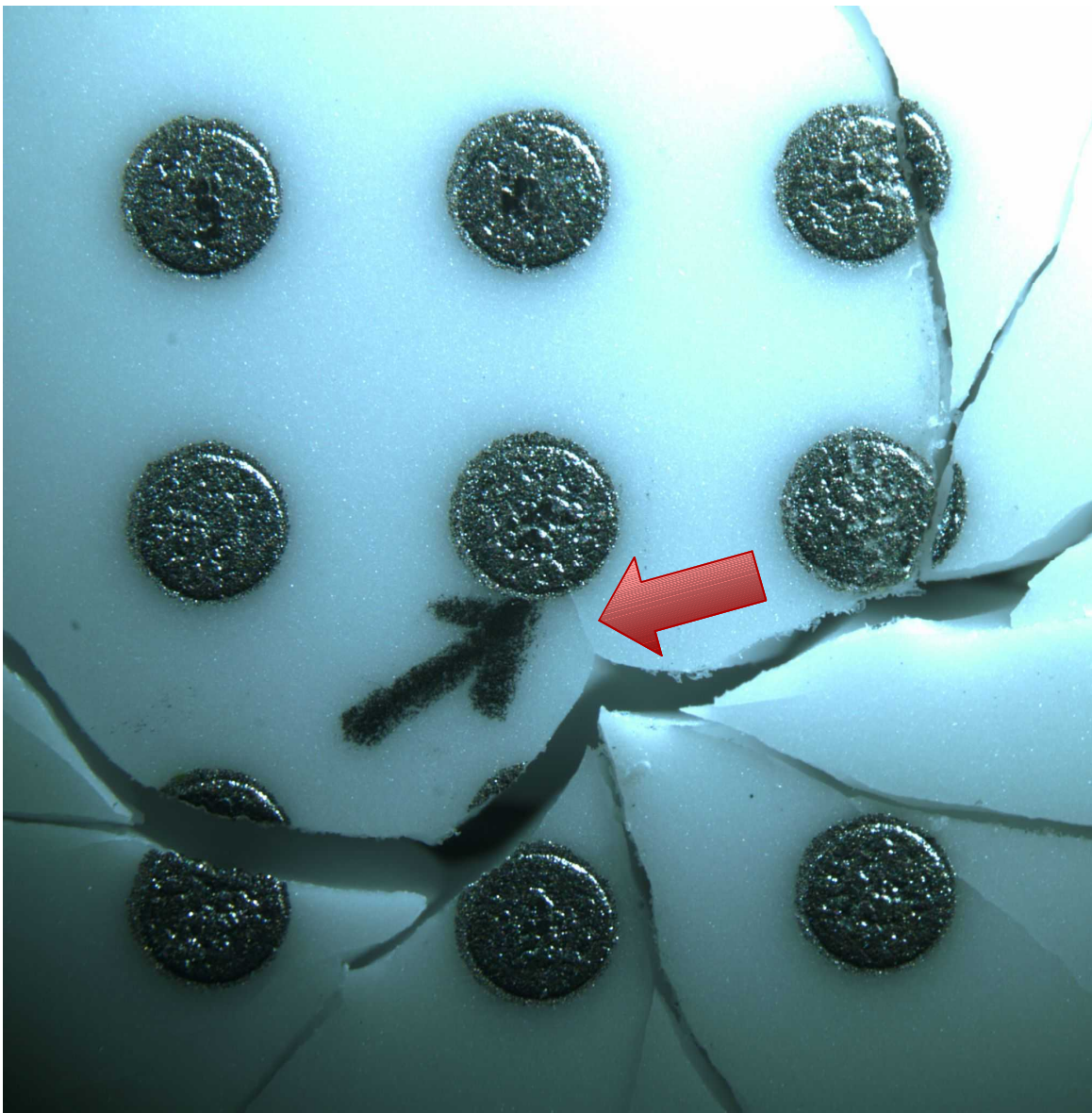
The failure origin has shifted: All failures are from the via

Phase II – Strength Lower

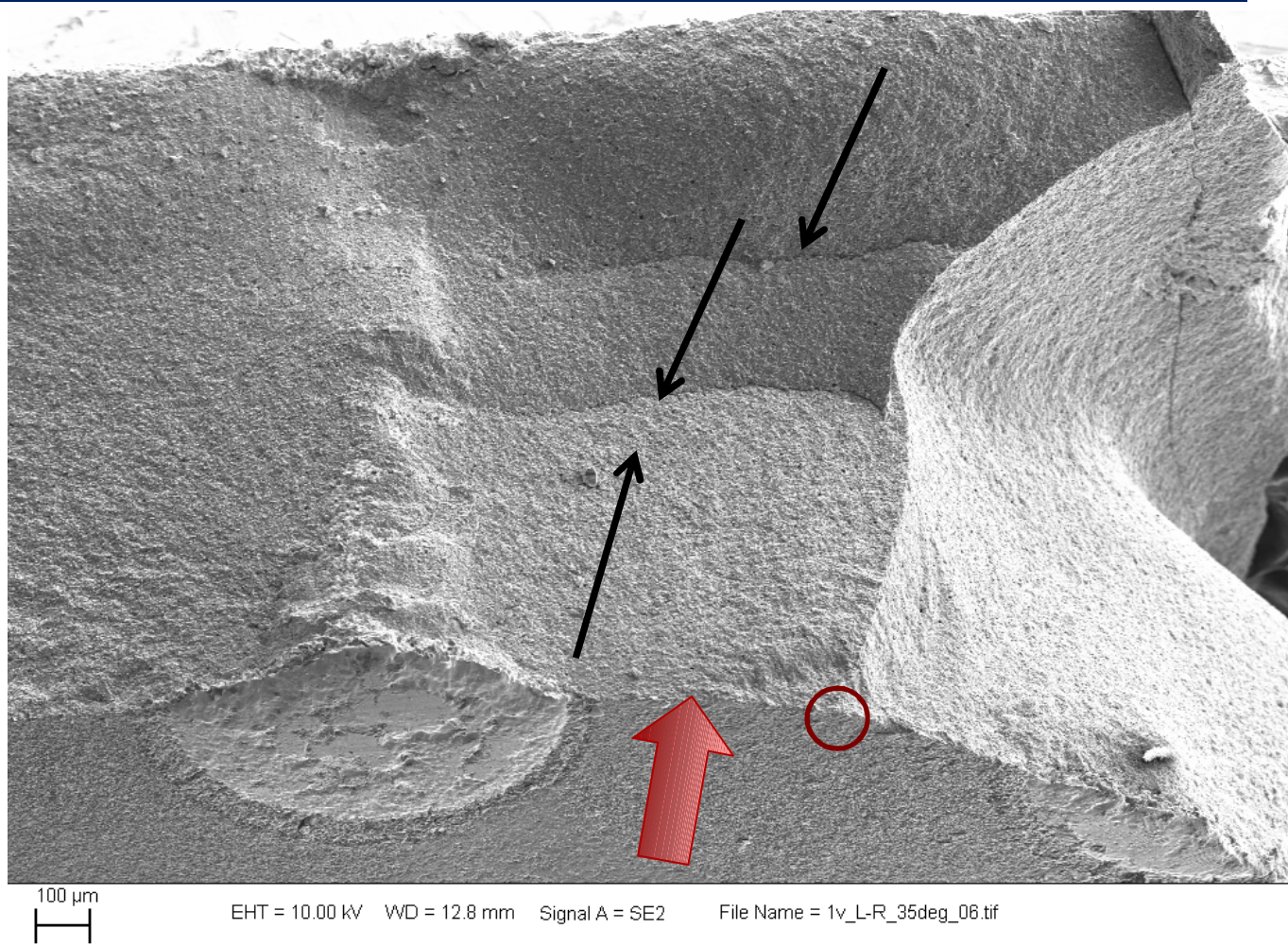


Phase II – Fractography (radial cracks)

Via 20 MPa/s
20% RH



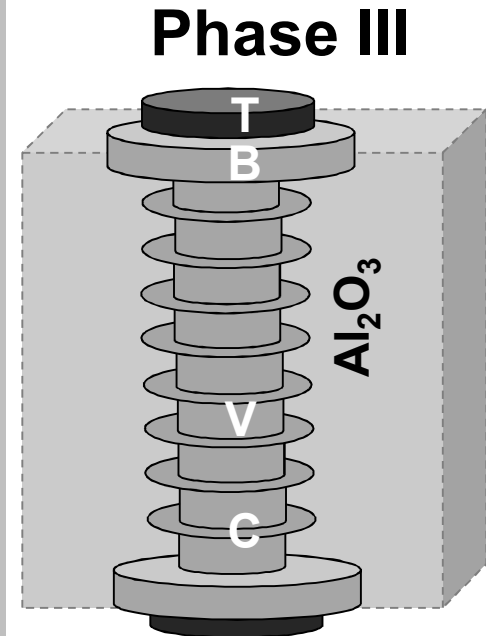
Phase II – Fractography (radial cracks)



These samples must have a small circumferential tensile stress near the vias: Radial cracks and slightly lower strength Lamination ?

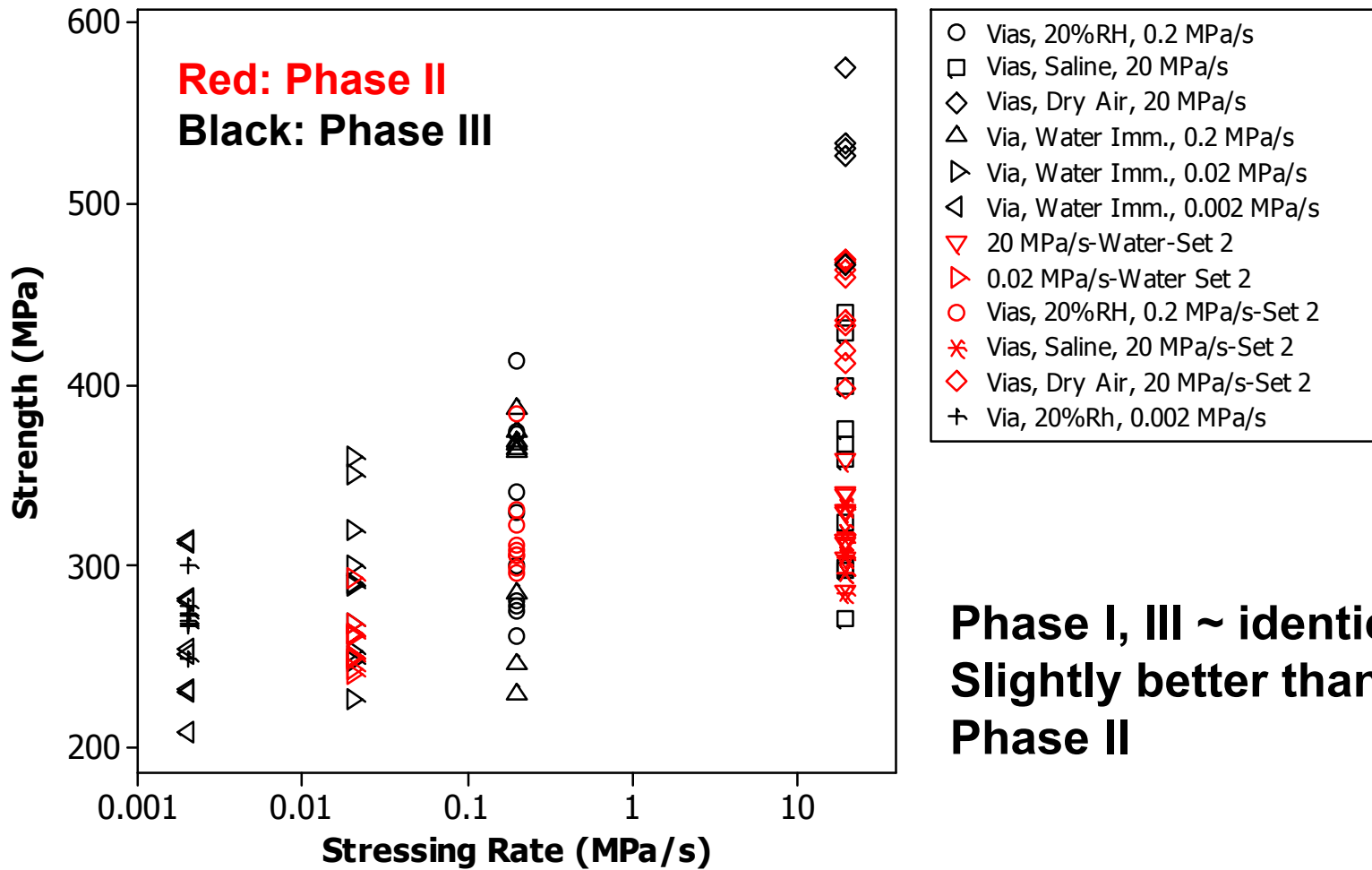
Via Materials Optimization – Phase III

- Significant process modifications (lamination, printing, order)
- 75/25 blend of fine/coarse Pt
- Compatible metal paste vehicle

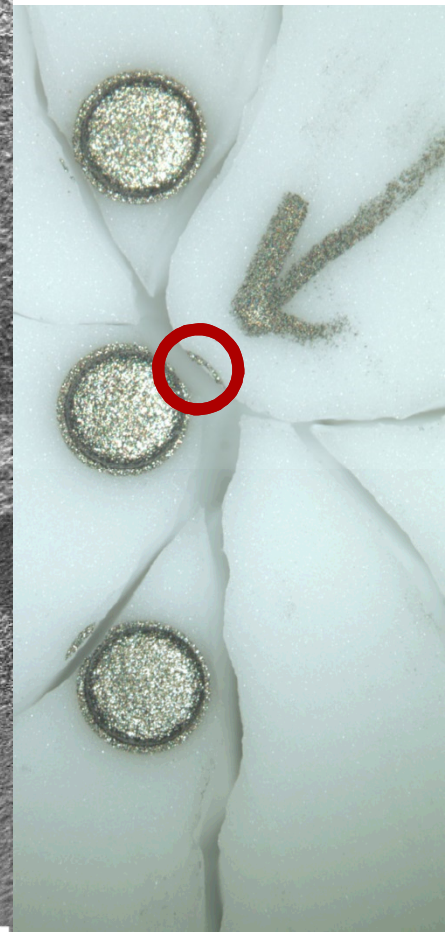
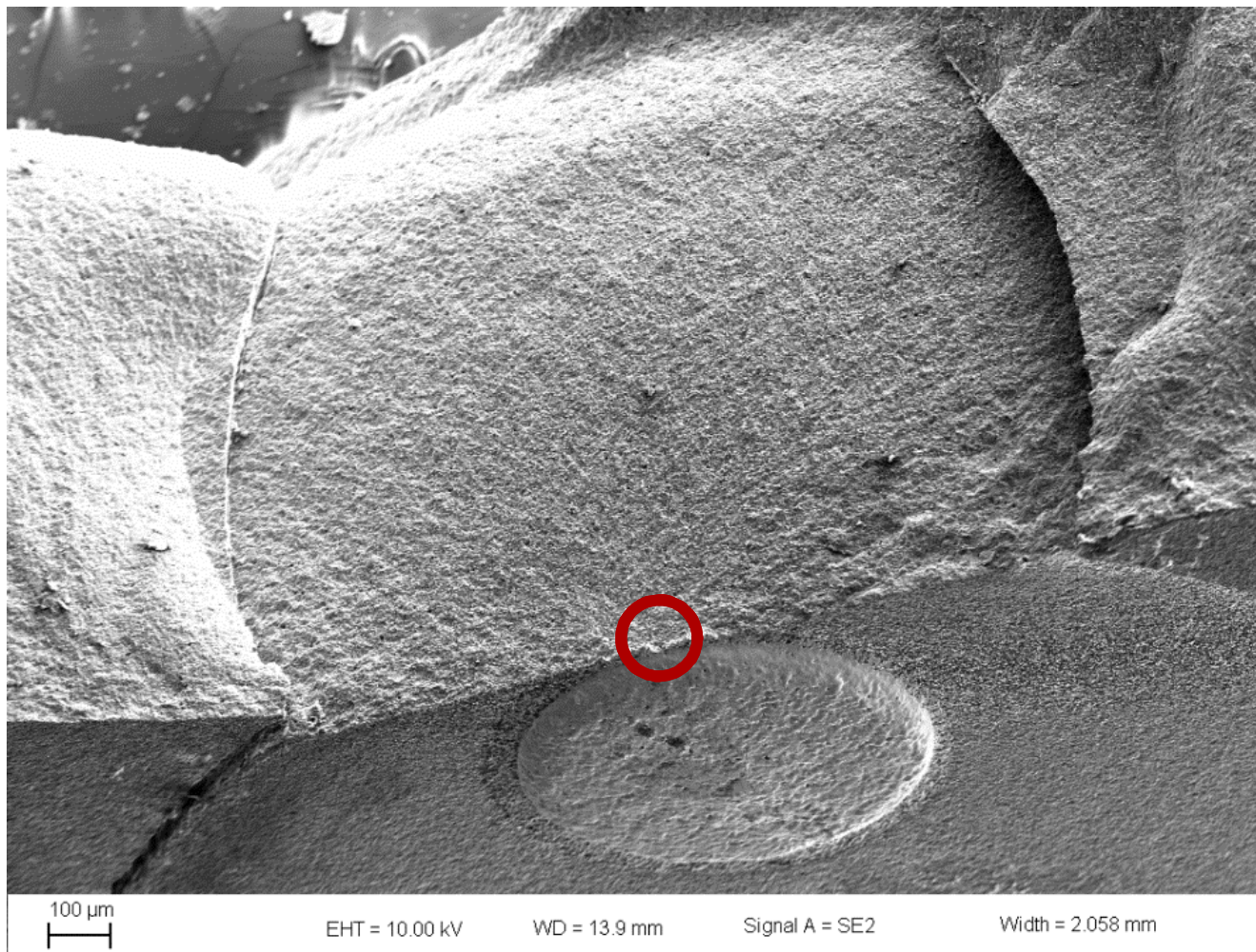


Top Pad (T)	100% Pt _f	50 Pt _f / 50% Pt _c	75 Pt _f / 25% Pt _c + 5% Al ₂ O ₃
Base Pad (B)	-	50 Pt _f / 50% Pt _c + 5% Al ₂ O ₃	75 Pt _f / 25% Pt _c + 5% Al ₂ O ₃
Via (V)	Pt + 5% (CaO, SiO ₂ , MgO, Al ₂ O ₃)	50 Pt _f / 50% Pt _c + 5% Al ₂ O ₃	75 Pt _f / 25% Pt _c + 5% Al ₂ O ₃
Cover Pads(C)	Pt + 5% Al ₂ O ₃	50 Pt _f / 50% Pt _c + 5% Al ₂ O ₃	75 Pt _f / 25% Pt _c + 5% Al ₂ O ₃

Phase III – Strength ~ base alumina



Phase III - Fractography



Conclusions

Strength:

Materials in Phase I, III had ~ identical strength; Phase II slightly lower

Notable exception of saline immersion, Phase I

- Vulnerability must be considered, tested for, and designed out prior to use

Stress State around the via (plasticity and thermal expansion considerations):

Phase I has a slight radial tension, and failure along interface in depth

- Removal of higher expansion glass phase led to redress of interfacial failure mode

Phase II has a slight circumferential tension, and radial cracking

Phase III has ~ 0 radial tensile stress

Lifetime:

Parameters extracted from these tests, and stresses use geometry, were used to calculate lifetimes > 20 years

Overall:

We can obtain material with vias that have similar lifetimes as base alumina material.

Failure Modes and Mechanics of Fracture in Co-Fired Engineering Ceramics

R. Tandon, Sandia National Laboratories, Albuquerque, NM 87123

Andrew Thom & Gordon Munns, Medtronic Inc., Minneapolis, MN 55430

Arne Knudsen, Kyocera America Inc., San Diego, CA 92123

Co-fired engineering ceramics can provide integration of multiple functions in one package, and lead to device miniaturization. Co-fired metals have thermal and elastic mismatches with the ceramic, producing local residual stresses which severely impact the fracture behavior and reliability. Observations and fracture analysis of a commercial low temp co-fired ceramic with gold vias show that while strength is reduced by as much as 60%, the susceptibility to sub-critical crack growth (SCG) is not lowered. A circumferential cracking mode around the vias has been observed in this system. Fracture mechanics solutions are derived to describe this failure mode, and correlated with fracture observations of crack kinking. In *in vivo* simulations of a commercial high temperature co-fired alumina ceramic-platinum via system, circumferential cracking is observed, but only at the slowest stressing rates. Processing changes made to these materials, which ultimately led to strength and SCG characteristics that were undistinguishable from the base materials, are described.

- Sandia National Laboratories is a multi-mission laboratory managed and operated by National Technology and Engineering Solutions of Sandia, LLC, a wholly owned subsidiary of Honeywell International, Inc., for the U.S. Department of Energy's National Nuclear Security Administration under contract DE-NA0003525.

Title: Failure analysis and sub-critical crack growth (SCG) characterization of Pt-Al₂O₃ high temperature co-fired (HTCC) ceramics

Abstract: Miniaturization and integration of multiple functions into one component is desired for device downsizing. HTCC alumina, with its high strength and bio-compatibility, provides an option for integration and higher reliability medical devices. A 92% alumina-platinum via HTCC material was characterized for failure modes and sub-critical crack growth, and modifications to processing were implemented to obtain a material with strength and SCG characteristics similar to bulk alumina. In phase I development, this material had strength equivalent to bulk alumina, except at low stressing rates in saline, body fluid-like environments, where a novel failure mode (circumferential cracking) was encountered. Processing changes implemented for Phase II materials led to failures emanating as radial cracks from the vias with slight loss of strength. Changes made to Phase III materials led to strength and SCG characteristics that were undistinguishable from the base materials. Fractographic evidence indicates that cracking originates tangentially to the via in Phase III material

Sandia National Laboratories is a multi-program laboratory managed and operated by Sandia Corporation, a wholly owned subsidiary of Lockheed Martin Corporation, for the U.S. Department of Energy's National Nuclear Security Administration under contract DE-AC04-94AL85000

Authors: Rajan Tandon, Clay S. Newton (Sandia), Andy Thom, Joyce Yamamoto, Markus Reiterer, and Gordon Munns (Medtronic); Hidekazu Otomaru, Hiroshi Matsumoto, Kengo Morioka, and Arne Knudsen, Kyocera North America Inc.